



The Roles of Stress-Activated Sty1 and Gcn2 Kinases and of the Protooncprotein Homologue Int6/eIF3e in Responses to Endogenous Oxidative Stress during Histidine Starvation

Naoki Nemoto^{1†}, Tsuyoshi Udagawa^{1†}, Takahiro Ohira^{1†}, Li Jiang², Kouji Hirota³, Caroline R. M. Wilkinson⁴, Jürg Bähler⁵, Nic Jones⁴, Kunihiro Ohta⁶, Ronald C. Wek^{2*} and Katsura Asano^{1*}

¹Molecular, Cellular, and Developmental Biology Program, Division of Biology, Kansas State University, Manhattan, KS 66506, USA

²Department of Biochemistry and Molecular Biology, Indiana University School of Medicine, Indianapolis, IN 46202, USA

³Shibata Distinguished Scientist Laboratory, RIKEN, Hirosawa 2-1, Wako-shi, Saitama 351-0198, Japan

⁴Cancer Research UK Cell Regulation Laboratory, Paterson Institute for Cancer Research, University of Manchester, Manchester M20 4BX, UK

⁵Department of Genetics, Evolution, and Environment, and UCL Cancer Institute, University College London, London WC1E 6BT, UK

⁶Department of Life Sciences, Graduate School of Arts and Sciences, University of Tokyo, Komaba 3-8-1, Meguroku, Tokyo 153-8902, Japan

Received 29 April 2010;
received in revised form
31 August 2010;
accepted 8 September 2010

Edited by J. Karn

Keywords:

amino acid control response;
oxidative stress;
Int6/eIF3e;
Gcn2;
MAP kinase

In fission yeast, Sty1 and Gcn2 are important protein kinases that regulate gene expression in response to amino acid starvation. The translation factor subunit Int6/eIF3e promotes Sty1-dependent response by increasing the abundance of Atf1, a transcription factor targeted by Sty1. While Gcn2 promotes expression of amino acid biosynthesis enzymes, the mechanism and function of Sty1 activation and Int6/eIF3e involvement during this nutrient stress are not understood. Here we show that mutants lacking *sty1*⁺ or *gcn2*⁺ display reduced viabilities during histidine depletion stress in a manner suppressible by the antioxidant *N*-acetyl cysteine, suggesting that these protein kinases function to alleviate endogenous oxidative damage generated during nutrient starvation. Int6/eIF3e also promotes cell viability by a mechanism involving the stimulation of Sty1 response to oxidative damage. In further support of these observations, microarray data suggest that, during histidine starvation, *int6*Δ increases the duration of Sty1-activated gene expression linked to oxidative stress due to the initial attenuation of Sty1-dependent transcription. Moreover, loss of *gcn2* induces the expression of a new set of genes not activated in wild-type cells starved for histidine. These genes encode heatshock proteins, redox enzymes, and

*Corresponding authors. E-mail addresses: rwek@iupui.edu; kasano@ksu.edu.

† N.N., T.U., and T.O. contributed equally to this work.

Abbreviations used: eIF, eukaryotic initiation factor; eIF2K, eIF2α kinase; ISR, integrated stress response; MAPK, mitogen-activated protein kinase; MAP2K, MAPK kinase; 3AT, 3-aminotriazole; MMTV, mouse mammary tumor virus; NAC, *N*-acetyl cysteine; CFU, colony-forming units; EMM, Edinburgh minimal medium; CRE, cAMP response element; MNase, micrococcal nuclease.

proteins involved in mitochondrial maintenance, in agreement with the idea that oxidative stress is imposed on *gcn2Δ* cells. Furthermore, early Sty1 activation promotes rapid Gcn2 activation on histidine starvation. These results suggest that Gcn2, Sty1, and Int6/eIF3e are functionally integrated and cooperate to respond to oxidative stress generated during histidine starvation.

© 2010 Elsevier Ltd. All rights reserved.

Introduction

Translation initiation is an important target of stress-responsive pathways regulated by various physiological and environmental signals. Reduced translation allows cells to conserve energy coincident with an altered program of gene expression, which leads to the production of proteins that have the capacity to ameliorate stress-induced damage.¹ Genetic alteration of eukaryotic initiation factors (eIFs) can disrupt the appropriate responses to physiological signals and stresses, which can alter the etiology and treatment of many diseases, including cancer.²

One of the key factors that contribute to the onset of disease processes is oxidative stress resulting from changes in metabolic activities or environmental stress.³ Malignant tumorigenesis can involve the altered activities of eIF2 α kinases (eIF2Ks), which are thought to provide cancer cells with increased resistance to nutritional and hypoxic stresses.^{4,5} Activation of eIF2Ks not only represses global protein synthesis but preferentially enhances the translation of key transcription factors such as Atf4. Atf4 triggers the transcription of stress-related genes as part of the integrated stress response (ISR) and is involved in alleviating oxidative stress and in controlling nutrient uptake and metabolism, as well as apoptosis.^{6–8} eIF2Ks are conserved throughout eukaryotes. The unicellular model organism *Schizosaccharomyces pombe* encodes three of the conserved eIF2Ks—Gcn2, Hri1, and Hri2, each of which is implicated in responses to oxidative stress.^{9,10} Similar to the mammalian ISR, eIF2K activation in *Sc. pombe* and in another yeast, *Saccharomyces cerevisiae*, promotes the transcription of a common set of genes termed GAAC (general amino acid control).^{11,12}

In conjunction with eIF2Ks, evolutionarily conserved stress-activated mitogen-activated protein kinases (MAPKs), including *Sc. pombe* Sty1 (also known as Spc1 or Phh1), also respond to oxidative stress. Sty1 is activated via a conserved MAPK cascade, including the MAPK kinase (MAP2K) Wis1 and the MAP2K kinases Wis4 and Win1.¹³ Sty1 activation then leads to an enhanced stability of the Atf1 transcription factor via mechanisms involving Atf1 phosphorylation and increased Atf1 activity via a phosphorylation-independent process.^{14,15} As

a consequence, oxidative stress triggers the expression of a group of genes termed CESR (core environmental stress response), most of which are dependent on the Sty1/Atf1 pathway.¹⁶

We recently found that both Sty1 and Gcn2 protein kinases are required for the response of *Sc. pombe* to histidine starvation elicited by the drug 3-aminotriazole (3AT), and that Gcn2 facilitates an increased transcription of genes encoding amino acid biosynthetic enzymes in response to nutritional deficiency.¹² While the Sty1 MAPK pathway has been linked to oxidative, osmotic, and DNA-damaging conditions,¹⁶ activation of Sty1 in response to histidine starvation was somewhat surprising, given that amino acid starvation is not thought to cause oxidative damage and that Sty1 does not facilitate the transcription of amino acid biosynthetic genes.¹²

Interestingly, the Sty1-dependent response during nutrient starvation is promoted by Int6/eIF3e,¹² whose mammalian homologue is encoded by a frequent integration site of mouse mammary tumor virus (MMTV) termed *int-6*.¹⁷ *int-6* encodes the e-subunit of eIF3.¹⁸ Mammalian eIF3 is composed of 13 subunits (eIF3a–eIF3m) and serves as the scaffold for eIF2 and for the cap binding protein eIF4F, which assists the binding of the 40S ribosome to mRNA.¹⁹ Although truncated forms of Int6/eIF3e found in MMTV-integrated tumors are known to be oncogenic both *in vitro*^{20,21} and *in vivo*,²² the mechanism of tumorigenesis caused by Int6 misregulation remains elusive. *Sc. pombe* encodes 11 of the 13 subunits found in mammalian eIF3.^{23–25} *int6*⁺ is not essential in fission yeast, but its loss (*int6Δ*) reduces translation initiation in yeast cultured in minimal media.^{12,23} This finding is in agreement with the important roles of eIF3e in translation initiation in mammalian cells.^{26,27} *Sc. pombe* Int6/eIF3e promotes the Sty1-dependent response, at least in part, by stimulating the expression of *atf1*⁺ by translational or posttranslational processes.¹²

In this study, we explored the integration between the Sty1/Atf1 MAPK pathway and key translational regulators (eIF2Ks and Int6/eIF3e) in the control of gene expression and cell viability during nutrient stress. Our results suggest that, during histidine starvation, Sty1 and Gcn2 cooperate to alleviate endogenous oxidative damage, which might be generated by a change in nutrient status. Further-

more, evidence that Int6/eIF3e modulates the Sty1 response to oxidative damage is provided. Our results support the model that alleviating oxidative damage during canonical nutritional stress is an important function of the integrated Sty1, Int6/eIF3e, and eIF2K stress response pathways. These findings provide insight into the cellular roles of eIF2Ks during nutrient deprivation and provide clues to understanding the mechanism by which MMTV integration at the murine *int-6* locus can contribute to tumorigenesis.

Results

Histidine starvation, as induced by 3AT, directly promotes Sty1-directed transcription

3AT is a potent inhibitor of the histidine biosynthesis enzyme imidazole glycerol phosphate dehydratase (encoded by *Sc. pombe* His5), causing histidine starvation in an otherwise prototrophic strain. Because 3AT is also suggested to inhibit other enzymes, such as catalase,²⁸ we wished to test if CESR is induced specifically by histidine starvation. For this purpose, we treated cells with 3AT in the presence or in the absence of added histidine. We then measured the accumulation of four representative CESR transcripts (*atf1*⁺, *pcr1*⁺, *cta1*⁺, and *gpd1*⁺ mRNAs) by Northern blot analysis (Fig. 1). As described above, Atf1 is a basic leucine zipper factor that is responsible for mediating many Sty1-dependent transcriptional events; Pcr1 is a second basic

leucine zipper factor that forms heterodimers with Atf1 and is also required for the expression of a number of Sty1-dependent genes;^{14,15,29,30} *cta1*⁺ encodes the major catalase activity induced by various Sty1-activating signals;¹⁶ and Gpd1 is a glycerol-3-phosphate dehydrogenase that produces glycerol in response to osmotic stress.³¹ The addition of histidine completely eliminated the accumulation of these four transcripts, which were induced with 30 mM 3AT in wild-type cells (Fig. 1). Together with our previous finding that the 3AT sensitivity of the *sty1* mutant is completely alleviated by addition of histidine,¹² these results endorse the specific effect of 3AT on the His5 enzyme in this yeast and further suggest that histidine starvation, rather than inhibition of catalase or other enzymes, directly promotes CESR transcription under 3AT-induced stress.

Sty1 MAPK cascade, Gcn2, and Int6/eIF3e appear to alleviate oxidative stress generated during 3AT-induced starvation

In order to gain insight into the mechanism whereby Sty1 is activated by 3AT-induced histidine starvation, we examined the involvement of other components of the Sty1 MAPK signaling pathway (Fig. 2a), which were previously linked with oxidative stress. Thus, we tested the 3AT sensitivity of mutant strains defective for Wis1 MAP2K, Wis4/Win1 MAP2K kinase, Mpr1/Mcs4 phosphorelay proteins, Mak1/Mak2/Mak3 histidine kinases,¹³ and the glycolytic enzyme Tdh1³² (Fig. 2b; T.O. and K.A., unpublished data). Among these mutants, those deleted for *mcs4*⁺, *wis1*⁺, or *wis4*⁺ were 3AT

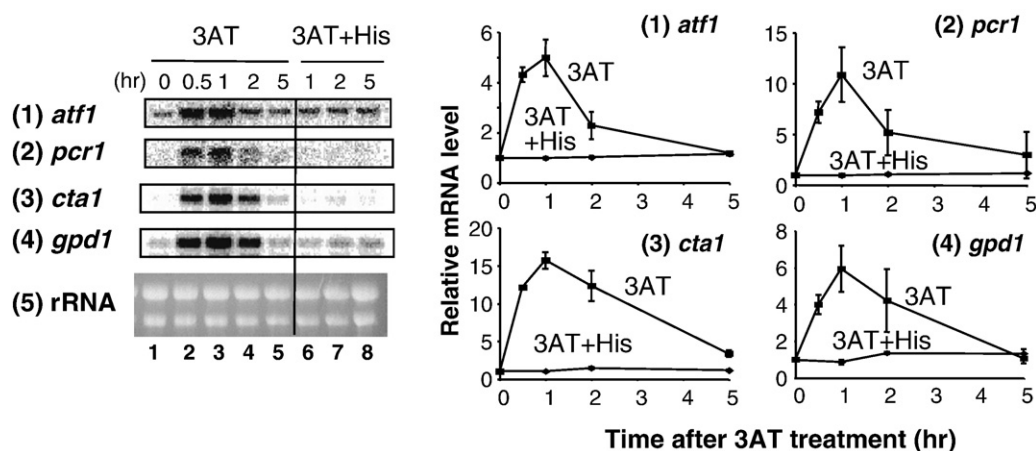


Fig. 1. Effect of histidine on 3AT-induced CESR transcription. A wild-type strain (KAY641) was grown exponentially in EMM-C-His and split into two cultures. One was starved for histidine by adding 30 mM 3AT (lanes 1–5), and the other was supplemented with 30 mM 3AT and 60 mM histidine simultaneously (lanes 6–8). Portions of the culture were withdrawn at indicated times, and mRNA levels were analyzed by Northern blot analysis using probes specific for genes listed to the left. Ethidium bromide staining of rRNA was included as loading control.¹² Graphs to the right show the time course for the levels of indicated mRNAs compared to the value at time 0 (1) (lane 1), with bars indicating standard deviation ($n = 2$). In the graph for 3AT+His, error bars are smaller than the size of the symbols.

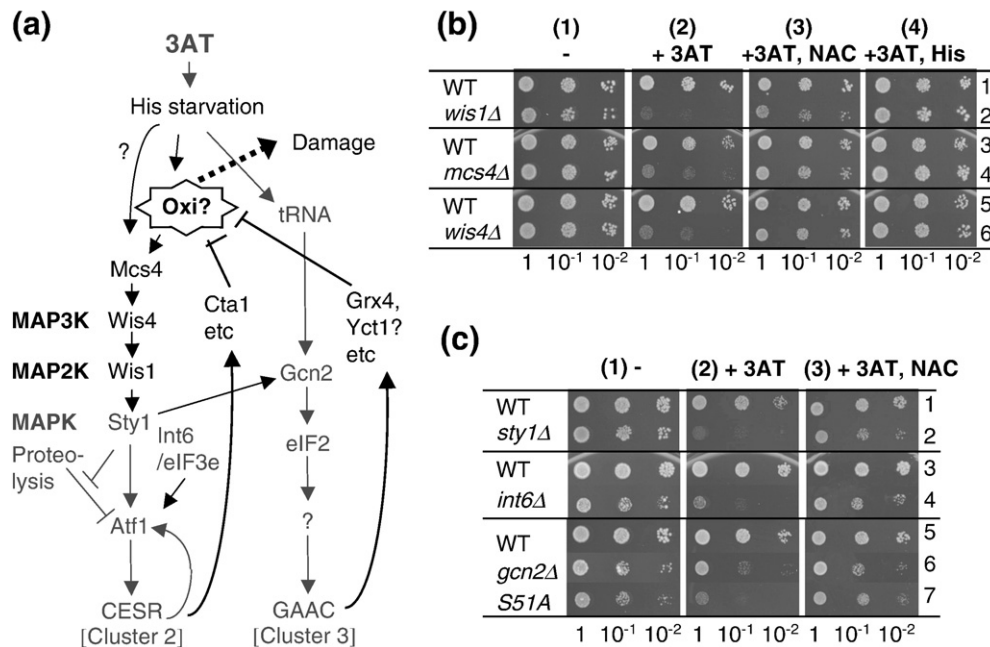


Fig. 2. Genetic evidence that a canonical Sty1 pathway, Int6/eIF3e, and Gcn2 specifically promote oxidative stress response during histidine starvation. (a) Model of 3AT-induced Sty1 and Gcn2 pathways in fission yeast. 3AT-induced histidine (His) starvation activates not only the Gcn2-dependent pathway (cluster 3, right column) but also the Sty1-dependent pathway (cluster 2, left column). Here it is proposed that at least one of the Sty1-activating signals is endogenous oxidation (Oxi), which would cause cellular damage (Damage) if the products of both pathways cannot antagonize the oxidative reagents (stopped bars towards Oxi?). This model was modified from the original model described by Udagawa *et al.*¹² Dark-gray letters and lines indicate a part of the pathways suggested by previous studies.¹² Black letters and lines indicate a part of the pathway suggested from this study. (b and c) Effect of NAC on the 3AT sensitivity of different mutants. The cultures of the indicated mutants and their wild-type (WT) controls were diluted to an A_{600} of 0.15; 5 μ l of this dilution and 10-fold serial dilutions was spotted onto EMM plus adenine agar plates not supplemented (1) or supplemented with 5 mM 3AT (2), 5 mM 3AT and 20 mM NAC (3), or 5 mM 3AT and 10 mM histidine (His) ((4) in (a)). However, for rows 5 and 6 in (b), we used 8 mM 3AT, 40 mM NAC, and 16 mM histidine. Plates were incubated for 4 days (1 and 4) and 6–7 days (2 and 3). Here we used minimal medium without amino acid supplements to promote the incorporation of NAC and histidine. The strains used in (b) are JP3 (row 1), JP260 (row 2), KAY793 (row 3), KAY794 (row 4), KAY456 (row 5), and KAY852 (row 6); in (c), we used KAY641 (rows 1 and 3), KAY640 (row 2), KAY647 (row 4), WY764 (row 5), KAY406 (row 6), and JP436 (row 7) (Table 1).

sensitive in a manner reversed by histidine (Fig. 2b). Therefore, a canonical MAPK cascade leading to Sty1 activation is required for survival upon 3AT exposure, as illustrated in Fig. 2a.

Because a major function of the canonical Sty1 MAPK cascade is to ameliorate oxidative damage, we hypothesized that the 3AT-induced Int6/eIF3e-assisted Sty1 pathway is also expressed to this end. In an effort to test this model, we used the antioxidant *N*-acetyl cysteine (NAC). As expected, NAC rescued the slow growth of the strains deleted for *sty1*⁺ or *int6*⁺ in the presence of 3AT in dilution assays (Fig. 2c, compare (2) and (3), rows 2 and 4). Likewise, NAC rescued the 3AT sensitivity of the mutants deleted for *mcs4*⁺, *wis1*⁺, or *wis4*⁺ (Fig. 2b). We previously showed that *sty1*⁺ and *int6*⁺ do not simply increase the expression of histidine biosynthesis enzymes;¹² otherwise, NAC would not rescue the 3AT sensitivity of the cells deleted for these

genes. Thus, the 3AT sensitivities of *sty1Δ* and *int6Δ* cells, and most likely those of other Sty1 pathway mutants, could be due to a failure of these mutant strains to respond to endogenous oxidative stress that might accompany histidine starvation.

In light of these findings, we also examined if NAC rescues the 3AT sensitivity of *gcn2Δ* cells; to our surprise, we found that it did, albeit partially (Fig. 2c, row 6). This suggests that Gcn2 functions to ameliorate oxidative damage. In order to test if the sensitivity of *gcn2Δ* cells is due to a failure in Gcn2 phosphorylation of eIF2 α , we tested the 3AT sensitivity of the mutant cells altering the eIF2 α phosphorylation site Ser51 to alanine (*sui2-S51A*).³³ The *sui2-S51A* strain is also 3AT sensitive in a manner suppressible by NAC (Fig. 2c). These findings suggest that phosphorylation of eIF2 α by Gcn2 is also important for alleviating oxidative stress during amino acid starvation.

Sty1 MAPK rescues cell death and genetic reversion during histidine starvation in a manner reversed by an antioxidant

While the major biological function of NAC is to act as an antioxidant, NAC or its cellular product (reduced glutathione) has other biological functions. To address whether NAC rescues the 3AT sensitivity of tested mutants by ameliorating cellular (oxidative) damage, we examined whether 3AT directly reduces the viability of the mutant cells and, if so, whether NAC reverses this effect. For this purpose, we grew yeast in semiexponential phase for several days by successive inoculation into fresh media in the presence or in the absence of 3AT (Fig. S1), and quantified cell viability at different times.

We first measured the survival of wild-type and *sty1* Δ cells following culturing for 1–5 days in 10 mM

3AT medium supplemented with histidine or NAC. Following the culture period, the cells were spotted onto a rich medium to measure cell viability (Fig. 3a). There was no significant loss of viability in the wild-type cells treated with 3AT for up to 5 days (Fig. 3a and b), even though 3AT substantially reduces the growth rate of these cells (Fig. S1). In contrast, only ~1% of *sty1* Δ cells survived a 2-day treatment with 3AT (Fig. 3a). Importantly, the reduced viability during this period was suppressed by the addition of histidine, emphasizing that starvation for this amino acid was central for the enhanced lethality accompanying the 3AT treatment of the *sty1* Δ strain. Interestingly, the viability of *sty1* Δ cells that was reduced after 2 days of starvation increased to ~100% on day 5 (Fig. 3a). As an illustration of this point, the *sty1* Δ cells that were recovered after 5 days of starvation grew faster on YES medium (Fig. 3a).

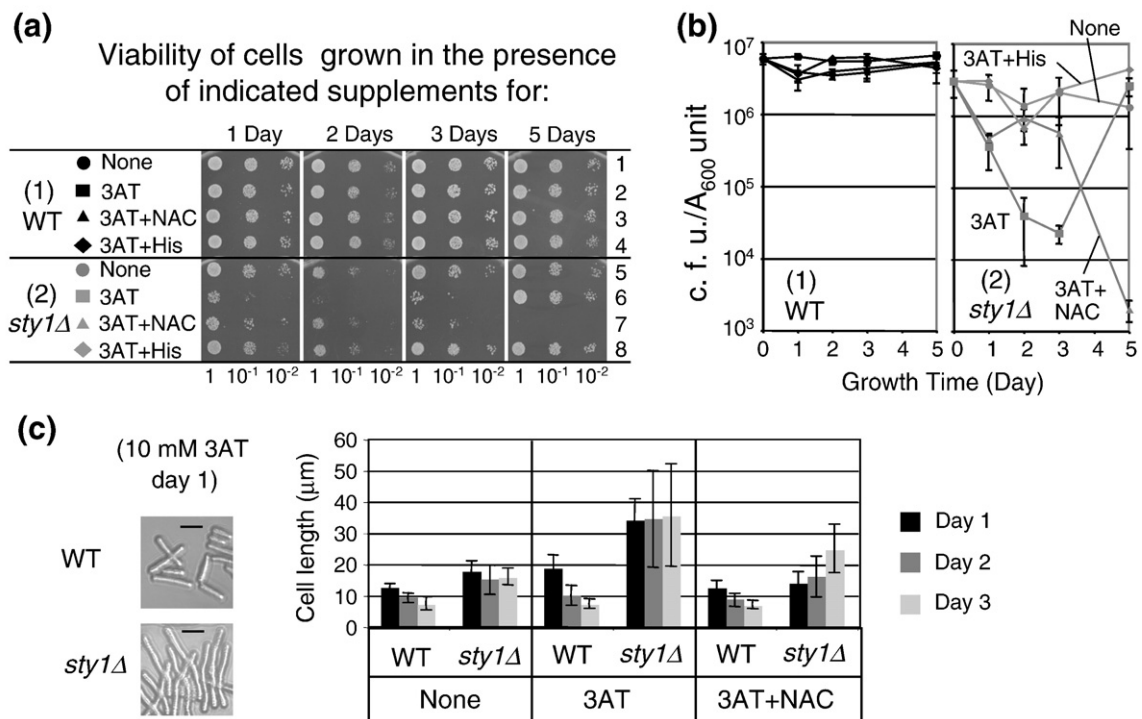


Fig. 3. Sty1 MAPK suppresses stress-induced death and mutagenesis during histidine starvation. (a) Viability assays in the presence of 10 mM 3AT. Fresh overnight cultures of KAY641 (wild type; black symbols) and KAY640 (*sty1* Δ ; gray symbols) were inoculated into ~3 ml of liquid EMM + Ade medium with 40 mM NAC, 20 mM histidine, and 10 mM 3AT, as indicated. The cultures were started at an A_{600} of ~0.3 with constant agitation at 30 °C, and the aliquots were periodically removed to measure the titer by spotting onto the YES agar plates (which were incubated at 30 °C for 2 days) and photographed. Colonies formed on each spot were counted to determine viability, as presented by CFU/ A_{600} . If two or more serially diluted spots contained well-dispersed colonies, the CFU/ A_{600} values obtained from each spot were averaged to determine the viability for that condition. Three independent viability assays were performed. (b) Graphs show the viabilities (CFU/ A_{600} unit culture) of wild-type (1) and *sty1* Δ (2) cells exposed to starvation for the times indicated. Bars indicate standard deviation ($n = 3$, except that a single experiment was performed with the control 3AT + His treatment). (c) Effect of 3AT and NAC on cell size. Photographs show the wild-type and *sty1* Δ cells under the designated growth conditions, with bars indicating 10 μ m. Portions of these cell cultures were withdrawn at the indicated times (see legend to the right) and observed under a microscope after fixing with formaldehyde. The graph indicates the average sizes of 20 different cells (μ m), which were measured with ImageJ software. The bars in the graph indicate standard deviation.

This finding suggests that after three or more days of starvation, the *sty1* Δ culture generated genetic mutants resistant to 3AT. In support of this idea, a sensitivity assay using 3AT-containing plates confirmed that about 10% of the *sty1* Δ cells that were recovered following 2 days of starvation were resistant to 3AT, whereas nearly 100% of the *sty1* Δ cells that survived after 3 days and 5 days of starvation were resistant to 3AT (data not shown).

In an effort to examine if the reduced viability is due to oxidative stress, we tested the effect of the antioxidant NAC. Its addition to the *sty1* Δ cells enhanced viability for up to 3 days of 3AT treatment (Fig. 3a). However, on day 5, there was reduced survival of the *sty1* Δ cells in the combined 3AT+NAC treatment (Fig. 3a). At this point, the addition of NAC to the 3AT liquid medium also suppressed the generation of 3AT-resistant cells, which instead caused the extinction of the entire culture on day 5 (Fig. 3b). These results suggest that *sty1*⁺ function contributes to a significant delay in cell death induced by oxidative stress during histidine starvation. NAC can provide some protection to *sty1* Δ cells against 3AT exposure for up to 3 days, but this antioxidant is not sufficient for longer treatment periods. In this sense, this shorter-term protection comes with a price. The 3AT-resistant revertants that accumulated in the *sty1* Δ cultures were absent when NAC was combined with 3AT in the medium (Fig. 3b).

sty1 Δ cells were longer during growth in the 10 mM 3AT medium (Fig. 3c), as observed under other stresses.³⁴ Thus, the observed decrease in colony-forming units (CFU) per A_{600} unit culture measured in Fig. 3c was potentially due to increased mass per cell and was as a consequence of plating fewer cells. However, this possibility was excluded by measuring the average size of wild-type and *sty1* Δ cells. Within the first 3 days of starvation, the size of the *sty1* Δ cells was only 2-fold to 4-fold larger than the size of wild-type cells in the 3AT medium, and NAC addition reduced the size of the *sty1* Δ cells by only <2-fold at each growth time (Fig. 3c).

These results together suggest that 3AT-induced histidine starvation imposes oxidative stress, and *sty1*⁺ rescues the stress likely by expressing CESR (Fig. 2a) (see Discussion also). In the absence of *sty1*⁺, the stress appears to damage the yeast cells, leading to reduced viability. The generation of 3AT-resistant cells could be due to DNA mutations or epigenetic changes. While the mechanism of this observation requires further examination, it is consistent with the idea that the cells grown in the presence of 3AT experience some sort of damage to chromosomes (indicated as "Damage" in Fig. 2a). The fact that NAC rescues the reduced viability of *sty1* Δ cells for the first 3 days (Fig. 3a and b) suggests that the damage is due to oxidative stress and, more importantly, agrees with the idea that the

major function of the Sty1 pathway, in this context, is to respond to oxidative stress.

Int6/eIF3e and Gcn2 eIF2K also suppress cell death during histidine starvation

We next addressed whether Int6/eIF3e and Gcn2 suppress cell death during histidine starvation, as observed for Sty1. We initially carried out the experiment using 10 mM 3AT in Edinburgh minimal medium (EMM), as performed previously (Fig. 3). However, the mutants deleted for *int6*⁺ or *gcn2*⁺ did not display a reduced viability even when incubated for up to 7 days (data not shown). Thus, we incubated the mutants in the medium containing 30 mM 3AT. Under these conditions, the wild-type yeast grew even more slowly than in the presence of 10 mM 3AT; after day 2, they almost stopped growing (Fig. S1b, (1)). Coincidentally, the viability of wild-type cells dropped to ~15% in the 3AT medium during this period (Fig. 4a and b, (1)). In contrast, there was a significant reduction in the viability of *int6* Δ cells (~1% survival) after 3 days of 3AT exposure (Fig. 4a and b, (2)). The viability of *gcn2* Δ cells also dropped more greatly (~10% survival) than the viability of wild type after 3 days ($p=0.05$, $n=4$) and 5 days ($p=0.03$, $n=3$) of 3AT exposure (Fig. 4a and b, (3)). This minor effect is consistent with the partial suppression of the 3AT sensitivity of *gcn2* Δ cells by NAC, as observed in dilution assays (Fig. 2c). As with *sty1* Δ cells, NAC enhanced the viability of *int6* Δ and *gcn2* Δ cells. Neither deletion resulted in a dramatic alteration in cell size during the experiments (Fig. 4c), reinforcing the idea that the differences observed in the CFU are due to cell death. These results suggest that Int6/eIF3e and Gcn2 are also required for suppressing cell death caused by histidine starvation, which likely results from oxidative damage.

As before for the *sty1* Δ strain, we did find that, after 5 days of 3AT treatment, nearly all *int6* Δ cells had been rendered resistant to 3AT. By contrast, the *gcn2* Δ cells, which are defective for the eIF2K pathway, remained 3AT sensitive (data not shown). These results suggest that histidine starvation induced cellular damage leading to genetic reversion, specifically in the absence of the Sty1 MAPK pathway or of the suggested adjunct regulator Int6 (Fig. 2a).

Int6/eIF3e is required for H₂O₂-induced oxidative stress

To strengthen the idea that Int6/eIF3e is involved in endogenous oxidative stress induced by histidine starvation, we wished to determine if Int6/eIF3e is involved in stimulating the Sty1 pathway directly under H₂O₂-induced oxidative stress. Dilution assays in Fig. 5a indicated that *int6* Δ substantially

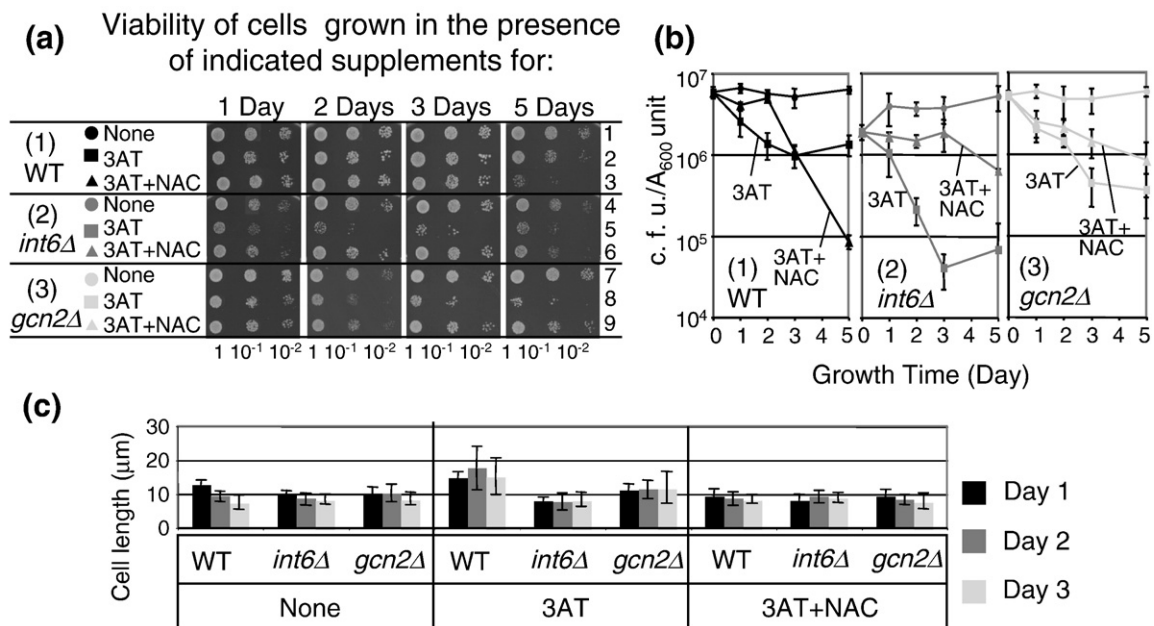


Fig. 4. Int6/eIF3e and Gcn2 promote viability during histidine starvation. (a and b) Viability assays in the presence of 30 mM 3AT. KAY641 (WT; black symbols; (1)), KAY647 (*int6Δ*; gray symbols; (2)), and KAY406 (*gcn2Δ*; light gray symbols; (3)) were grown exponentially with 120 mM NAC and 30 mM 3AT, as indicated, and assayed for viability, all as in Fig. 3a and b. (b) The time course of cell viability ($n = 3$) was presented as in Fig. 3b. (c) Effect on cell size. The cultures of the cells used in (a) and (b) were withdrawn on the indicated day and measured for cell sizes as in Fig. 3c.

increased sensitivity to continuous H₂O₂ exposure in three different genetic backgrounds (rows 1 and 2, *h⁹⁰ ade6-M216*; rows 3 and 4, *h⁻ ade6-M216*; rows 5–7, *h⁻*), as *sty1Δ* did, albeit more strongly (Fig. 5a). To directly test if *int6Δ* reduced viability during exposure to H₂O₂ for a defined period, we treated the strains to high levels of H₂O₂ (1–4 mM) for 4 h and examined their viability after plating on YES medium agar plates. The *int6Δ* cells were sensitive to exposure to 1 mM H₂O₂, while the majority of wild-type cells tolerated this level of exposure (Fig. 5b). Thus, Int6/eIF3e is involved in oxidative damage response.

To examine the effect of *int6Δ* on Atf1-dependent CESR transcription during H₂O₂-induced stress, we performed Northern blot analysis to determine the mRNA levels of several key CESR genes (*atf1*, *pcr1*, *cta1*, and *gpd1*) from wild-type or *int6Δ* strains following exposure to 2 mM H₂O₂ for up to 180 min. In wild-type cells exposed to H₂O₂, there were increased levels of each of the transcripts (Fig. 5a and d). For each CESR gene, *int6Δ* delayed and attenuated their accumulation. We also observed that *int6Δ* reduced the abundance of Atf1 protein prior to applying stress (Fig. 5e). The reduced abundance of Atf1 protein was not accompanied by a change in *atf1⁺* mRNA levels (Fig. 5e), suggesting that *int6⁺* promotes *atf1⁺* expression at the posttranscriptional level in a complex-rich

medium, as well as in a minimal medium.¹² Thus, the diminished CESR transcription observed in *int6Δ* cells could at least partially result from the lowered abundance of Atf1 protein. These results indicate that *int6⁺* is also required for the response to H₂O₂-induced oxidative stress by a mechanism involving the regulation of *atf1⁺* expression.

Int6/eIF3e, but not eIF3h, plays a role in rescuing histidine starvation by enhancing *atf1⁺* expression

At this point, that Int6/eIF3e and the Sty1 pathway are commonly involved in oxidative stress and that Int6/eIF3e enhances the expression of *atf1⁺* encoding the transcription factor targeted by Sty1 are evidences relating Int6/eIF3e and the Sty1 pathway.¹² To establish the genetic relationship between *int6⁺* and *atf1⁺* during histidine starvation, we performed a complementation assay. Figure 6a indicates that the 3AT sensitivity of the *int6Δ* mutant was partially suppressed by overexpression of Atf1 and, as expected, by overexpression of Int6/eIF3e. These results reinforce the idea that the enhanced expression of *atf1⁺* contributes to the resistance to histidine starvation conferred by *int6⁺* (Fig. 2a).

To determine if the 3AT sensitivity of the *int6Δ* mutant is a general consequence of eIF3 disruption, we created and characterized a yeast mutant deleted for *eif3h⁺* encoding the h-subunit of eIF3. The *eif3hΔ*

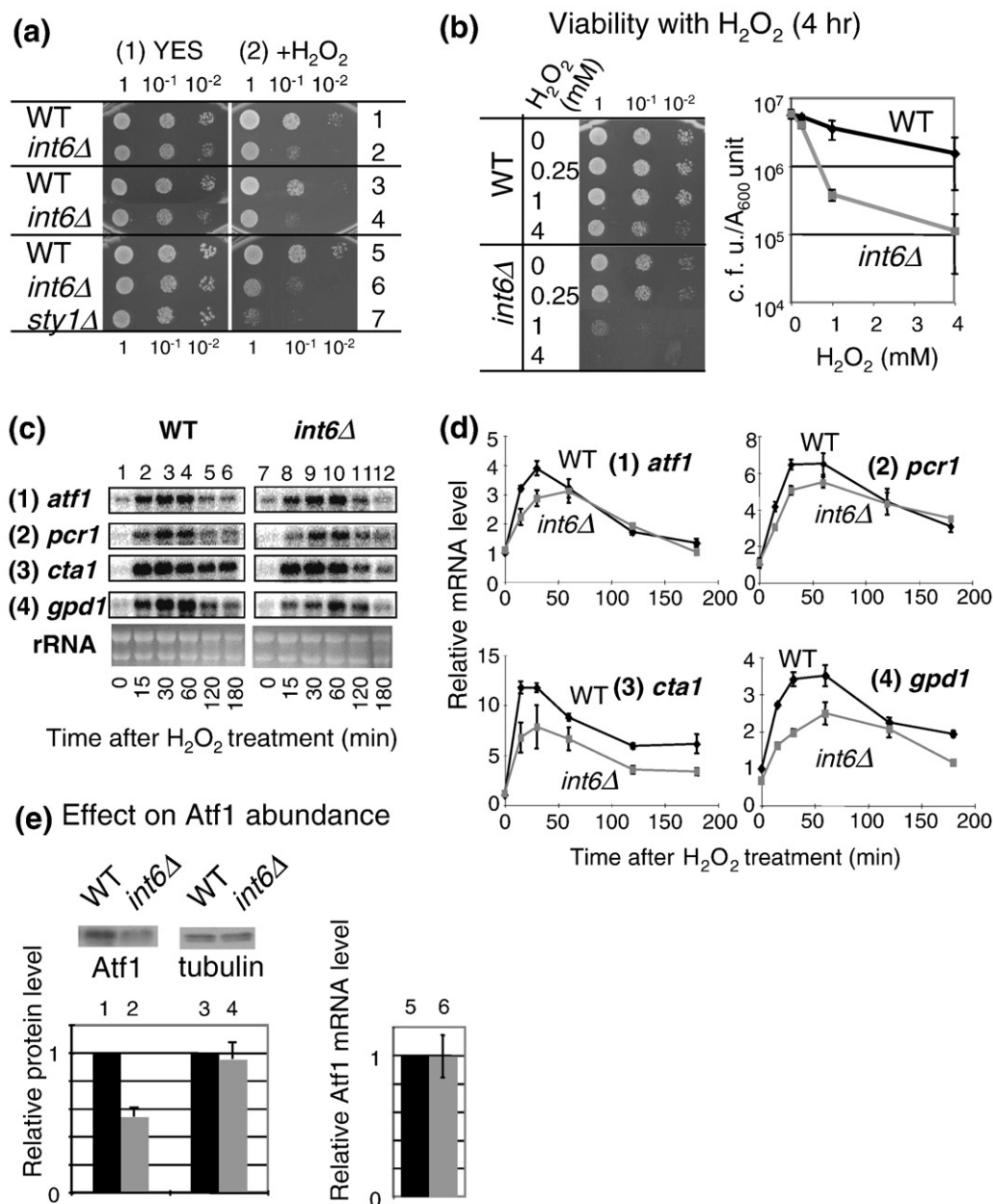


Fig. 5. Int6/eIF3e stimulates H₂O₂-induced oxidative stress response. (a) Sensitivity test: Cultures of wild-type (WT), *int6*Δ, or *sty1*Δ*sty1*Δ strains were diluted and spotted onto YES medium alone (1) or with 1 mM H₂O₂ (2), and grown for 2 days. Included in this sensitivity test are strains KAY456 (row 1), KAY508 (row 2), WY764 (row 3), KAY252 (row 4), KAY641 (row 5), KAY647 (row 6), and KAY640 (row 7). (b) Viability test: Strains KAY456 (WT) and KAY508 (*int6*Δ) were grown to an A₆₀₀ of 0.5, and then H₂O₂ was added at the indicated final concentrations. After incubation for 4 h, samples were taken, diluted, and spotted onto YES agar plates, and the plate was incubated for 2 days. The graph describes the plot of viability (CFU/A₆₀₀ culture) against the exposed H₂O₂ dose, with bars indicating standard deviation (*n* = 3). (c and d) Effect on CESR transcription: Strains WY764 (WT) and KAY252 (*int6*Δ) were cultured in YES medium with 2 mM H₂O₂ for the indicated times (min), and RNA was prepared and analyzed by Northern blot analysis using probes specific for the genes indicated to the left. The bottom panels show ethidium-bromide-stained rRNAs, which were included as loading controls. Graphs in (d) show the intensity of the transcript bands shown in (c), compared to the value for wild type at time 0 of H₂O₂ treatment. Graphs present the average from two independent experiments. (e) WY764 (WT) and KAY252 (*int6*Δ) were grown to an exponential phase in YES medium and analyzed by immunoblotting using affinity-purified anti-Atf1¹⁵ and anti-tubulin (Sigma) antibodies, as indicated. The graph indicates the levels of Atf1 and tubulin proteins (columns 1–4), averaged from two independent experiments, and *atf1* mRNA (columns 5 and 6; averaged from *n* = 4) in wild-type versus *int6*Δ cells, with bars indicating standard deviation.

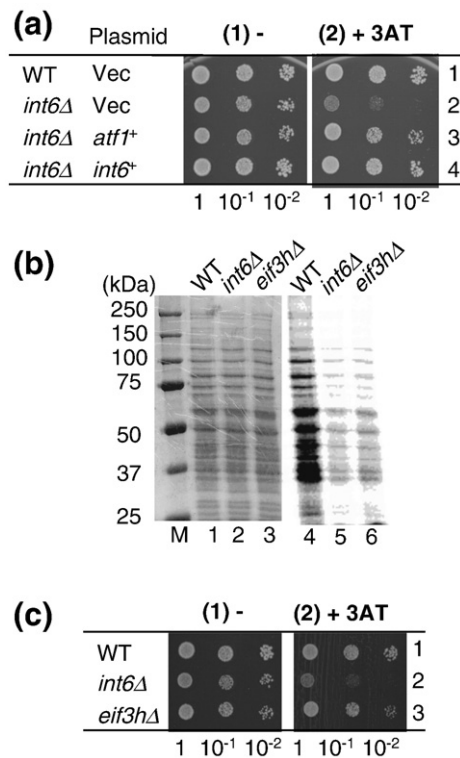


Fig. 6. Int6/eIF3e, but not eIF3h, is involved in the regulation of *atf1*⁺ expression. (a) Complementation assay. Wild type (WT; KAY586) or *int6Δ* (KAY587) transformed with pREP41X (Vec), pREP41X-*atf1* (*atf1*⁺),¹⁵ or pREP-int6 (*int6*⁺)²³ was spotted on EMM-C-His-Leu medium alone (1) or with 4 mM 3AT (2), and grown for 4 days or 6 days, respectively. (b and c) 3AT sensitivity and the total protein synthesis of WT (KAY641), *int6Δ* (KAY647), and *eif3hΔ* mutant (KAY649). In (b), the cells were grown exponentially in EMM, cultured with [³⁵S]Met for 20 min, and collected, and protein lysates were prepared. Five micrograms of total proteins was resolved by SDS-PAGE, stained by Coomassie blue (lanes 1–3; M, size standards), and analyzed by the STORM PhosphorImager (lanes 4–6). (c) 3AT sensitivity was assayed on plates containing EMM-C-His alone (1) or supplemented with 5 mM 3AT (2), and the plates were incubated for 4 days and 6 days, respectively. Because *int6Δ* and *eif3hΔ* mutants grew slowly on the minimal agar plate but less so on the complete defined medium, EMM-C.¹²

strain, like *int6Δ*, substantially reduced the total protein synthesis rate compared to wild type, as measured by [³⁵S]Met incorporation into total proteins (Fig. 6b, Table 1). Equal Coomassie staining of the total proteins indicates equal protein loading in this experiment (Fig. 6b, lanes 1–3). The reduction in protein synthesis was accompanied by an increase in doubling time (Table 1). Despite this fact, the *eif3hΔ* strain did not confer 3AT sensitivity (Fig. 6c). Therefore, 3AT sensitivity is a specific

Table 1. Effect of *eif3hΔ* and *int6Δ* on total protein synthesis and growth rate

Strain	Genotype	Total protein synthesis (%) ^a	Doubling time (min) ^b
KAY641	Wild type	(100)	156 ± 4
KAY647	<i>int6Δ</i>	18 ± 1	207 ± 35
KAY649	<i>eif3hΔ</i>	29 ± 5	187 ± 23

^a ³⁵S incorporation into proteins throughout each lane in the autoradiograph (examples shown in Fig. 6b, lanes 4–6) was determined by the STORM PhosphorImager and compared to the value for wild type (in parentheses; average of three independent experiments).

^b The doubling time of each strain was measured in liquid EMM at 30 °C (average of four independent experiments).

phenotype associated with the loss of the Int6/eIF3e subunit (see Discussion).

Transcriptional evidence for a feedback mechanism within Int6/eIF3e-assisted Sty1-dependent response caused by histidine starvation

Having gained evidence suggesting that Int6/eIF3e rescues oxidative damage during 3AT-induced starvation, we focused on our previous Northern blot studies indicating that *int6Δ* not only decreases the initial rate of CESR transcript (*atf1*⁺, *pcr1*⁺, *gpd1*⁺, and *cta1*⁺, as used in Fig. 1) accumulation upon exposure to 30 mM 3AT but also allows extended accumulation of these transcripts, which peaks after 3 h of 3AT treatment¹² (also see Fig. S2). This extended transcriptional response was accompanied by the extended duration of Wis1-directed Sty1 activation.¹² Thus, the delayed and extended CESR transcription appears to indicate an increasing oxidative signal that can activate Sty1 even in *int6Δ* cells and eventually damage the cells.

To verify these trends at a genomewide level, we examined the transcriptional microarray data of 3AT-treated *int6Δ* cells. Of the 169 CESR transcripts induced by 30 mM 3AT (termed cluster 2 genes by Udagawa *et al.*¹²), the abundance of 85% of these mRNAs (144 genes) was lower in *int6Δ* cells than in wild type after 1 h of 3AT addition, in agreement with their slower accumulation. Conversely, the abundance of 51% of these transcripts (87 genes) was higher in *int6Δ* cells than in wild type after 3 h of 3AT addition. Again, this is in agreement with the delayed accumulation. Together, expression of 61 CESR genes showed the combined lower expression at 1 h and higher expression at 3 h in *int6Δ* cells after 3AT addition. This pattern is in agreement with the delayed and extended CESR transcription suggested by our Northern blot experiments.¹²

To address if *int6Δ* extends the duration of Atf1 transcriptional activity rather than, for example, the

stability of the transcripts, we examined changes in chromatin structure at an Atf1-binding site [cAMP response element (CRE)].³⁵ We chose *cta3*⁺, which

encodes a P-type ATPase cation pump, because its expression was strongly enhanced after 3 h of stress application (Fig. 7a and b). As shown in Fig. 7c,

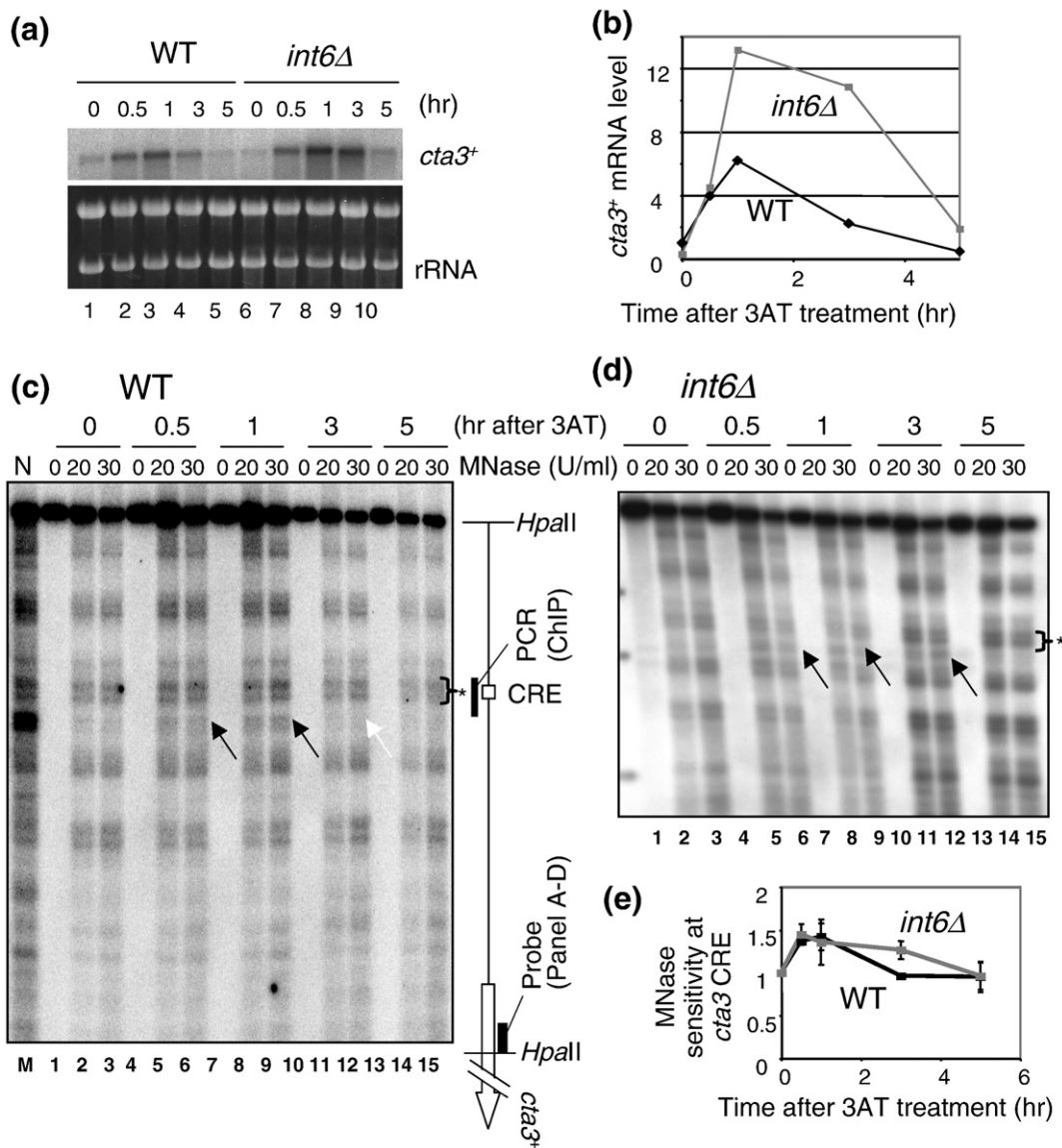


Fig. 7. Direct effect of *int6Δ* on Atf1 activity at its binding site upstream of *cta3*⁺. (a and b) Effect of *int6Δ* on 3AT-induced *cta3*⁺ mRNA levels. Strains WY764 (WT) and KAY252 (*int6Δ*) were grown in the presence of 3AT, withdrawn at the indicated times, and analyzed by Northern blot analysis using a [³²P]*cta3* probe, as described in Fig. 1. The autoradiography generated from Northern blot analysis is illustrated in the top panel (and ethidium bromide staining of rRNA was included as loading control; bottom panel). The graph in (b) presents the mRNA levels relative to wild type at time 0. (c and d) Changes in the nucleosome structure at *cta3*⁺ CRE. The crude chromatin fractions from wild-type (c) and *int6Δ* (d) cells treated with 3AT for the indicated times were partially digested with MNase at the concentrations listed at the top of the panel. DNA was prepared and analyzed by Southern blot analysis, as described in Experimental Procedures. Black arrows indicate MNase cleavage sites enhanced by 3AT treatment. The white arrow indicates the cleavage site, which disappeared in wild-type DNA after 3 h of treatment. The schematic to the right of (c) describes the location of the CRE, the DNA fragments mentioned, and the *cta3*⁺ open reading frame. N, naked DNA treated with MNase. (e) The graph indicates the time course of the intensity of MNase cleavage at the *cta3*⁺ CRE (arrows in c and d) relative to that of the unchanged cleavage site (asterisks in c and d) in wild-type (black symbols) and *int6Δ* (gray symbols) cells. The intensity of cleavage was averaged from lanes with 20 U/ml and 30 U/ml MNase; bars indicate the standard deviation from two independent measurements.

micrococcal nuclease (MNase) sensitivity at a site near the *cta3* CRE, indicative of the nucleosome remodeling therein, was increased at 0.5–1 h after 3AT treatment in wild-type cells (arrows in the gel), coincident with the accumulation of *cta3* mRNA and other CESR mRNA (Fig. 7a and b). In *int6*Δ cells, the remodeling of the area near *cta3* CRE lasted longer and could be observed after 3 h of 3AT treatment (Fig. 7d, arrows; for quantification of MNase sensitivity, see also Fig. 7e), again coinciding with the abundance of *cta3* mRNA (Fig. 7a and b). Thus, *int6*Δ extends the duration of remodeling of an Atf1-dependent gene during histidine starvation. Chromatin immunoprecipitation confirmed that Atf1 actually binds the *cta3* CRE, although Atf1 was already bound to the CRE before the stress, as observed for other CREs,¹⁴ and the increase in Atf1 binding by 3AT treatment was minor although significant (K.H., K.A., and K.O., unpublished data; see [Experimental Procedures](#)).

Together with our previous report,¹² these results support the idea that a Sty1-activating signal, most likely oxidative stress, builds up within 3AT-treated *int6*Δ cells due to a failure to quickly antagonize the original (oxidative) stress, and that the increased signal in turn activates Sty1. Thus, our results also suggest that a feedback loop operates within the 3AT-induced Sty1 pathway, as illustrated in Fig. 2a. However, we could not determine whether the original Sty1-activating signal, which quickly activated Sty1 within 15 min of 3AT exposure,¹² is also an oxidative stress (see [Discussion](#)).

Transcriptional evidence that Gcn2 reduces oxidative stress during histidine starvation

In agreement with the relationship of *gcn2*⁺-regulated genes with oxidative stress, our cDNA microarray analysis indicated that 3AT-induced genes requiring *gcn2*⁺ (cluster 3¹²) include genes that potentially ameliorate oxidative damage, as listed in [Table 2](#). Grx4 is a nuclear glutaredoxin that antagonizes the oxidative damage of chromosomes.³⁶ SPAC1F12.06c encodes a predicted DNA repair endonuclease V, whereas SPCC18.09c encodes the yeast homologue of aprataxin, a human protein that binds damaged DNA and is involved in DNA repair.³⁷ The expression of *yct1*, encoding a potential cysteine transporter,³⁸ would favor glutathione synthesis. Furthermore, cluster 3 includes many predicted mitochondrial proteins, of which *mmf1*, *gor1*, and *atm1* are likely to be involved in mitochondrial maintenance ([Table 2](#)), based on studies of the homologous *Sa. cerevisiae* genes.^{39,40} In particular, the *Sa. cerevisiae* mutant deleted for *atm1*, encoding a Fe/S cluster precursor transporter, increases the level of glutathione, which protects against oxidative stress.⁴⁰ Thus, *gcn2*⁺ can promote the expression of genes involved in mitochondrial maintenance and biogenesis, which can influence oxidative damage (Fig. 2a).

If Gcn2 alleviates oxidative damage, the lack of *gcn2*⁺ would cause oxidative stress in the presence of 3AT, which might in turn express a specific response. To test this idea, we analyzed genes that are specifically induced in 3AT-treated *gcn2*Δ cells. Indeed, our reanalysis of the expression profiling

Table 2. 3AT-induced genes that are dependent on Gcn2 (cluster 3 in Udagawa *et al.*¹²) and potentially involved in oxidative stress response

Gene	Systematic name	Fold up in wild-type cells ^a	Fold up in <i>gcn2</i> Δ cells ^a	Description ^b
DNA repair genes				
<i>grx4</i>	SPAPB2B4.02	2.9	1.3	Nuclear glutaredoxin essential for viability
C1F12.06c	SPAC1F12.06c	2.7	1.0	DNA repair endonuclease V (predicted)
C18.09c	SPCC18.09c	3.0	1.2	Human aprataxin homolog
Cysteine transport				
<i>yct1</i>	SPCPB1C11.03	4.2	0.3	Cysteine transporter (predicted)
Mitochondrial genes				
<i>mmf1</i>	SPBC2G2.04c	3.9	0.8	YjgF family protein similar to <i>Sa. cerevisiae</i> Mmf1p, which is involved in mitochondrial DNA stability
<i>gor1</i>	SPBC1773.17c	2.5	0.5	Glyoxylate reductase (predicted)
<i>atm1</i>	SPAC15A10.01	4.7	0.9	Mitochondrial inner membrane component, ABC family iron transporter (predicted)
C3G6.05	SPAC3G6.05	3.2	1.2	Mvp17/PMP22 family protein 1, with a mitochondrial localization signal
C1235.11	SPCC1235.11	2.0	0.9	Mitochondrial protein, human BRP44L ortholog
C1259.09c	SPCC1259.09c	2.7	0.9	Probable pyruvate dehydrogenase protein × component, mitochondrial
Homocysteine synthesis				
<i>str3</i>	SPCC11E10.01	3.0	1.2	Cystathionine β-lyase (predicted)

^a Fold increase in mRNA abundance after 3 h of 3AT treatment, compared to the value in wild type at time 0.

^b Based on the Gene Ontology database, with relevant information from the *Sc. pombe* Gene Database added.

data of 3AT-treated *gcn2Δ* cells¹² revealed 217 genes, which are induced less than 2-fold in wild-type cells but induced more than 2-fold in *gcn2Δ* cells after 3 h of 3AT treatment. As shown in Fig. 8a, cluster analysis divided these genes into two groups, clusters 4 and 5, following the cluster numbers described previously.¹² Table S1 shows 121 genes belonging to clusters 4 and 5, which are not induced more than 2-fold in wild type

but induced by an even higher 2.4-fold in *gcn2Δ* cells treated with 30 mM 3AT. The genes in cluster 4 encode heatshock proteins, redox enzymes, and proteins involved in protein degradation and mitochondrial maintenance. Cluster 4 generally overlaps with stress genes, especially with oxidative stress genes ($p = 2 \times 10^{-24}$). The genes in this cluster also strongly overlap with cluster 7 genes (Fig. 2 in Chen *et al.*⁴¹) that

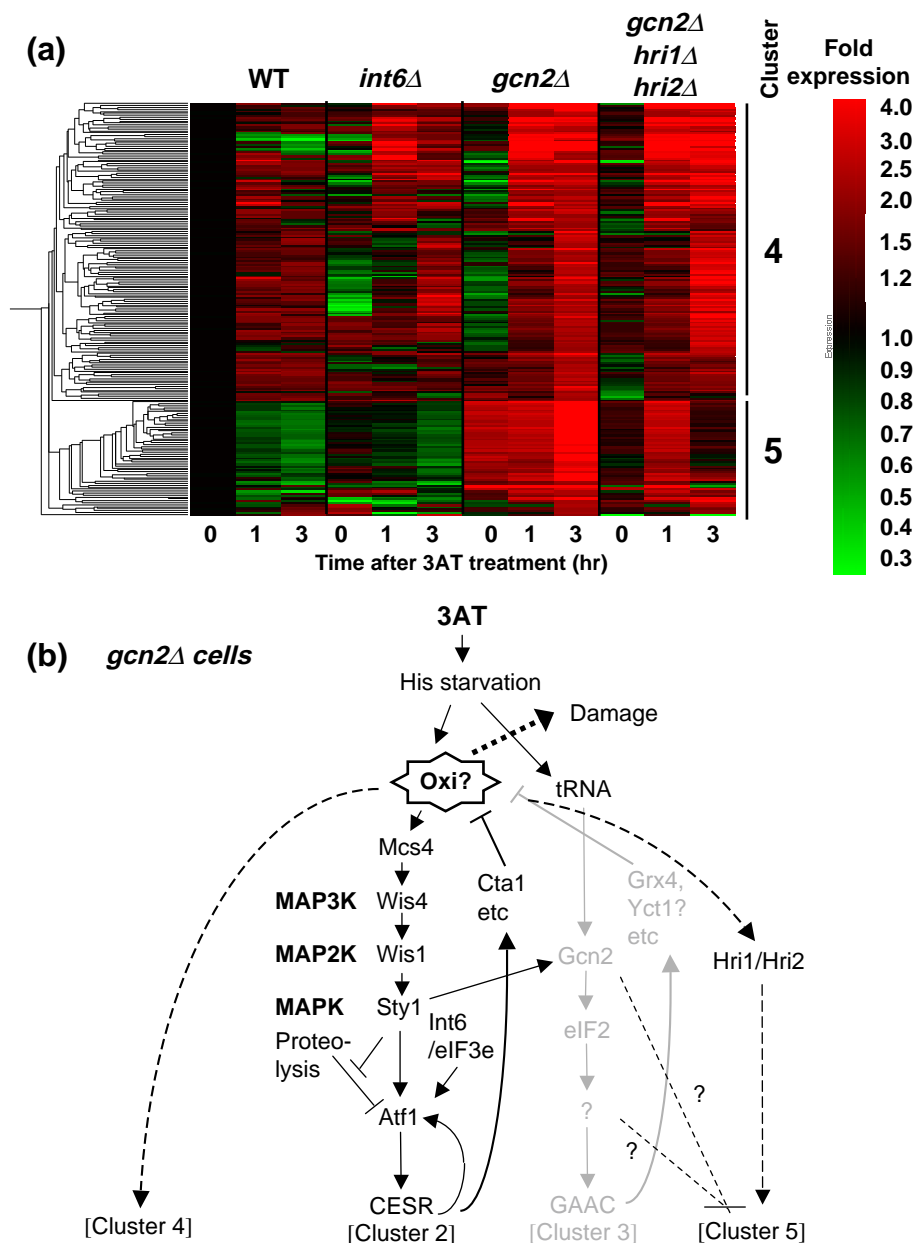


Fig. 8. Genes induced by 3AT specifically in the absence of *gcn2*⁺. (a) Clustering of 217 genes induced <2-fold in wild type and >2-fold in *gcn2Δ* cells by 30 mM 3AT,¹² with the level of expression presented by the red/green scale bar to the right. Each column represents the expression level of the genes in yeast carrying mutations indicated across the top after 3AT treatment for the time shown on the bottom. Bars and numbers to the right indicate the gene cluster identified. (b) Model of gene regulation within *gcn2Δ* cells. Black and gray drawings indicate the pathways proposed to be operated or shut down, respectively, in the cells. The model states that the absence of Gcn2 generates oxidative damage (Oxi?), which in turn induces clusters 4 and 5, with the latter repressed by *gcn2*⁺ and stimulated by *hri1*⁺/*hri2*⁺.

are strongly induced by two oxidative compounds, menadione and *t*-butylhydroperoxide (but not by hydrogen peroxide) ($p = 3 \times 10^{-12}$), and with a set of genes (Fig. 4a in Chen *et al.*⁴¹) whose transcription does not depend on a kinase or transcription factor known to drive the oxidative stress response, such as Sty1, Pmk1, Atf1, Pcr1, or Pap1 ($p = 2 \times 10^{-9}$). Thus, the observed expression of cluster 4 genes is consistent with the model that this novel set of genes responds to oxidative damage generated in *gcn2* Δ cells (Fig. 8b). Cluster 5 genes encode proteins that are involved in protein folding or degradation and mitochondrial maintenance, again consistent with the generation of oxidative stress (Table S1). However, this cluster does not overlap with any known gene list (see Fig. 8b and Discussion).

Sty1 MAPK stimulates Gcn2-dependent transcription by enhancing Gcn2 activation

We next examined the cross-talk between the Sty1 pathway and the Gcn2 pathway in 3AT-induced stress response. Immunoblotting with anti-phospho-

eIF2 α antibodies confirmed that Gcn2 phosphorylation of eIF2 α peaks between 30 min and 1 h of 3AT addition (Fig. 9a). Phosphorylation was absent when alanine was substituted for Ser51 of eIF2 α (Fig. 9a, (3)). Deletion of *gcn2*⁺ significantly delayed eIF2 α phosphorylation (Fig. 9a, (4)), suggesting that alternative eIF2Ks (Hri1 and/or Hri2) can partially compensate in response to 3AT. Importantly, the maximal Gcn2 phosphorylation of eIF2 α is preceded by Sty1 activation, which is at a maximum within the first 15 min of 3AT stress.¹² To test whether the early Sty1 activation can contribute to Gcn2 function, we examined the effect of *sty1* Δ on 3AT-induced eIF2 α phosphorylation and the attendant Gcn2-dependent transcription. We found that *sty1* Δ significantly delayed the Gcn2 phosphorylation of eIF2 α within the first 30 min of 3AT addition (Fig. 9a (2) and b). Moreover, *sty1* Δ significantly delayed Gcn2-dependent gene transcription accordingly (Fig. 9c); in wild-type cells, the accumulation of the three Gcn2 target transcripts peaked at 1 h of 3AT-induced starvation, the same time as for the CESR transcription. Loss of Sty1 diminished this early peak response and rather

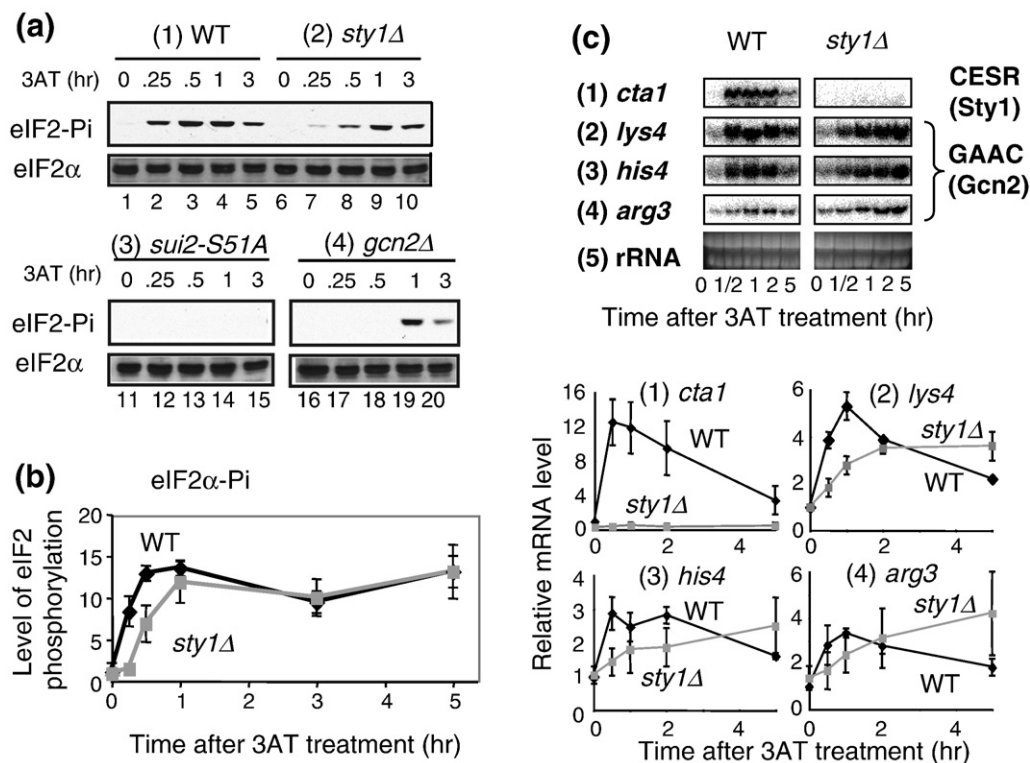


Fig. 9. Sty1 MAPK stimulates Gcn2 phosphorylation of eIF2 α . (a) eIF2 phosphorylation: Strains KAY641 (1), KAY640 (2), JP436 (3), and KAY406 (4) were grown in EMM-C-His to an early exponential phase, and then 30 mM 3AT was added. Cells were harvested and protein lysates were prepared and analyzed by immunoblotting with anti-phospho-eIF2 α (top) or total eIF2 α (bottom) antibodies, as described previously.⁹ (b) The graph shows the relative levels of phospho-eIF2 α normalized for total eIF2 α levels in the wild-type (black symbols) or *sty1* Δ (gray symbols) cells used in (a). The values are compared to the ratio calculated for wild type at time 0. Bars indicate standard deviation ($n = 3$ or more). (c) 3AT-induced transcript level changes were examined in strains KAY641 (wild type) and KAY640 (*sty1* Δ) for the genes indicated to the left, as described in Fig. 1.

enhanced Gcn2-dependent gene transcription later, especially after 5 h of starvation (Fig. 9c). These results indicate that *sty1*⁺ can promote rapid Gcn2-dependent eIF2 α phosphorylation and the attendant GAAC transcription during histidine starvation (Fig. 2a).

Because an increase in eIF2 α phosphorylation was observed in a *sty1* mutant,⁴² it was conceivable that the later enhancement of GAAC transcription in *sty1* Δ cells after 5 h of 3AT treatment was due to an increased level of eIF2 α phosphorylation. To test this idea, we examined eIF2 α phosphorylation until 5 h of 3AT treatment. However, *sty1* Δ did not alter the level of eIF2 α phosphorylation compared to wild type after 3–5 h of 3AT treatment (Fig. 9b). Thus, an additional factor contributes to the *sty1* Δ -induced enhancement of GAAC transcription.

Discussion

The evidence presented here—suggesting that oxidative stress response represents a major component of fission yeast response to 3AT-induced histidine starvation—is based on the viability assays of mutants deleted for the *sty1*⁺, *gcn2*⁺, and *int6*⁺ genes, which are directly involved in the response to 3AT-induced starvation (Figs. 3 and 4), as well as on transcriptional profiles (both Northern blot analysis and microarray), consistent with the expression of potential antioxidant genes at the timing expected for individual mutations (Figs. 1 and 7).¹² Although the addition of NAC complimented the reduced viability caused by 3AT-induced starvation (Figs. 3 and 4), NAC or its cellular product, reduced glutathione, can have functions other than antioxidant; thus, the experiments with NAC do not necessarily prove an antioxidant function. However, our ferric xylenol orange assay⁴³ recently showed that the lipid fractions isolated from wild-type *Sc. pombe*, which had been treated for 3–24 h with 3AT in the same medium as we have used here, were 2-fold to 3-fold more strongly peroxidized, and that NAC addition reduced this effect (N.N., Kimberly Hall, Yuka Ikeda, Ruth Welti, and K.A., unpublished data), in agreement with the idea that NAC indeed rescues oxidative damage within the 3AT-treated cells. Together with this finding and the transcriptional evidence indicating that *int6* Δ delays and extends the duration of Sty1 activation and the attendant transcription,¹² we propose that a feedback mechanism (as illustrated in Fig. 2a) operates within the Sty1 pathway, and that Int6/eIF3e plays an important role in this regulation.

The source of oxidative signals that lead to Sty1 activation under the feedback response is likely to be complex. An example of the internal source of oxidation would include oxidative degradation of metabolic compounds in peroxisomes, which requires a high catalase activity to detoxify gener-

ated H₂O₂ or a change in mitochondrial respiration status that can occur during a shift from anaerobic to aerobic conditions. In support of the mitochondria-derived oxidation, the importance of mitochondrial maintenance during histidine starvation is suggested by the possible Gcn2 regulation of genes involved in this process, both positively (cluster 3, Table 2) and negatively (cluster 5, Fig. 8; Table S1).

However, we could not obtain clues to help us understand the mechanism whereby the original starvation signal quickly promoted Sty1 activation and the attendant transcription, as observed in Fig. 1. In order to address this question, we examined the effect of NAC on 3AT-induced CESR transcription, but NAC had only a marginal effect on this robust transcriptional response (Fig. S2). This negative result rather suggests that Sty1 is rapidly activated by a feedforward mechanism without being mediated by an oxidative signal (“?” in Fig. 2a). A feedforward mechanism can evolve as a result of repeated changes in the environment.⁴⁴ Shiozaki *et al.* showed that carbon source starvation also activates the Sty1 MAPK cascade, in this case directly via Mcs4.⁴⁵ Thus, it would be important to determine whether the nutritional stress arrangements that lead to Sty1 activation commonly result in the generation of endogenous oxidative stress.

The role of Int6/eIF3e in the regulation of *atf1*⁺ gene expression

Here we also showed that *atf1*⁺ expression can rescue the 3AT sensitivity of an *int6* Δ mutant (Fig. 6a), reinforcing the concept that *int6*⁺ regulates *atf1*⁺. How does Int6/eIF3e regulate *atf1*⁺ expression? Int6/eIF3e is an important part of eIF3,^{23,24} promoting general protein synthesis (Fig. 6b, Table 1).¹² *atf1*⁺ mRNA has a relatively long 5' untranslated region of ~300 bp, devoid of any upstream open reading frames, which has been shown to be important for translational control of other mRNAs.⁴⁶ Given that Int6/eIF3e forms an interface with eIF4F in humans,²⁶ the intact eIF3 with this subunit might promote the translation of capped mRNAs with a relatively long 5' untranslated region, including *atf1*⁺ mRNA. An alternative model suggested by the specific effect of *int6* Δ on 3AT sensitivity, compared to that of *eif3h* Δ (Fig. 6b and c, Table 1), states that Int6/eIF3e more specifically interacts with a subset of mRNA, including *atf1*⁺ mRNA. Mass spectrometry analysis of human eIF3 indicates that eIF3e is located in proximity to the RNA-binding eIF3d subunit,^{47,48} raising the possibility that the eIF3e/eIF3d module can serve as an mRNA-regulatory unit of eIF3. Combined *sty1* Δ *int6* Δ strains show a stronger sensitivity to 3AT compared to single mutants,¹² suggesting that *int6*⁺ also regulates damage response pathway(s) other than the Sty1 pathway. Therefore, it would be

important to address the molecular basis of the regulation of *atf1*⁺ expression by Int6/eIF3e and to find additional targets regulated by this eIF3 subunit.

Potential role for Gcn2 in responses to endogenous oxidative stress during histidine starvation

Our suggestion that Gcn2 may play a role in antioxidation (Fig. 8, Table 2) is consistent with the finding that the mammalian ISR, governed by eIF2Ks, contributes to glutathione biosynthesis and resistance to oxidative stress.⁶ The expression of antioxidant clusters 4 and 5 in *gcn2*Δ cells (Fig. 8) provides additional evidence that the Gcn2-dependent response includes a response to oxidative stress during histidine starvation. Of interest were the cluster 5 genes whose expression is repressed by *gcn2*⁺ and induced in its absence in a manner dependent on *hri1*⁺ and *hri2*⁺ (Fig. 8). Hri eIF2 kinases possess a heme-binding site, which may be used to sense oxidative compounds.¹ In the absence of *gcn2*⁺, eIF2α is partially phosphorylated by 3AT treatment in a manner dependent on *hri1*⁺ and *hri2*⁺¹² (also see Fig. 9a, (4)). Thus, Hri1/Hri2 appear to be activated by oxidative stress, thereby stimulating the expression of cluster 5 by an unknown mechanism (Fig. 8b). As for the regulation of cluster 4, the gene induced most highly in *gcn2*Δ cells (by 12-fold) belongs to this cluster and encodes a potential transcription factor (Table S1) whose *Sa. cerevisiae* homolog, Mbf1p, is a coactivator of Gcn4p.⁴⁹ Thus, it would be intriguing to test whether this protein and an unidentified Gcn2 target facilitate the transcription of this set of genes.

Sty1-mediated activation of Gcn2 (Fig. 9) would couple the major stress-activated MAPK pathway to translational control. Because exogenous H₂O₂ does not induce GAAC transcription (T.U. and K. A., unpublished data), the coupling of Sty1 and Gcn2 appears to be restricted to specific stress arrangements, such as those involving nutrient starvation. Sty1 could activate Gcn2 directly or indirectly. The indirect mechanism may involve other signaling pathways known to respond to nutritional stresses, such as TOR protein kinase pathways, which are proposed to regulate *Sa. cerevisiae* Gcn2p^{50,51} and *Sc. pombe* Gcn2, specifically via Tor1.⁵² Extending the human relevance of this study, Thiaville *et al.* that a coupling of the extracellular signal-regulated kinase MAPK pathway and the Gcn2 pathway occurs following the amino acid limitation of human hepatoma cells.⁵³

Implication for cancer biology

Appropriate expression of antioxidation pathways is vital to tumor suppression.⁵⁴ For example, cells expressing activated H-Ras produce H₂O₂, and the resulting oxidative damage is ameliorated by the

human homologue of Sty1, p38, which suppresses H-Ras-activated tumorigenesis.⁵⁵ If the oxidative damage that we propose to be present in the *int6*Δ yeast mutant also occurs in mammalian cells with compromised Int6/eIF3e activity, this might facilitate tumorigenesis by a process involving DNA mutations elicited during oxidative damage.⁵⁴ In addition, nutrient limitation is suggested to occur with progression of solid tumors. Accordingly, recent studies highlight a prooncogenic role for eIF2Ks and the attendant ISR expression in securing sufficient nutrients and in alleviating oxidative damage.⁷ However, oxidative damage, when untreated by the MAPK and/or eIF2K pathway, may also compound tumorigenesis, enhancing genetic diversity that could contribute to the aggressiveness of tumors. Indeed, earlier studies implicated eIF2Ks in tumor suppression, and there is a strong correlation between up-regulation of protein synthesis and progress of tumorigenesis.² In light of this study, it would be intriguing to investigate the role of eIF2Ks and ISR-directed antioxidation in preventing tumor initiation.

Experimental Procedures

Yeast strains

The *Sc. pombe* strains used in this study are listed in Table 3. We used strains prototrophic for amino acid biosynthesis in order to address resistance to 3AT, an inhibitor of histidine synthesis. For this purpose, we used transformation with *leu1*⁺-encoding or *his7*⁺-encoding plasmids to convert the leucine and/or histidine auxotrophy of previously constructed strains. Accordingly, strains KAY793 and KAY794 are transformants of KS2096⁵⁶ and CA220,⁵⁷ respectively, carrying pREP41X (*leu1*⁺). KAY852 is a transformant of JM1505⁵⁸ carrying pREP41X (*leu1*⁺) and pEA500 (*his7*⁺).

KAY649 (*eif3h*Δ) was constructed by introducing the *eif3h*⁺ (SPAC821.05) disruption DNA, generated by PCR using oligos eIF3h-FW and eIF3h-RV (Table 4) and pKS-FA-ura4 (provided by Y. Watanabe, University of Tokyo) as template. pKS-FA-ura4 is a derivative of pKS-ura4⁵⁹ carrying the same primer-binding site as those of pFA6a derivatives. The resulting disruption DNA carries *ura4*⁺ in a reverse orientation relative to *eif3h*⁺. The integration of the disruption DNA into *eif3h*⁺ was confirmed by PCR using a pair of oligonucleotides, with one binding to a chromosomal site outside of the region present in the *eif3h*⁺ disruption DNA and with the other binding to the *ura4*⁺ coding region, namely eIF3h-up and *ura4*-midF, and eIF3h-down and *ura4*-midR, respectively (Table 4).

KAY586 was prepared by converting the *ura4-D18* locus of JY879 (*h*⁹⁰ *ade6-M210 leu1-32 ura4-D18*) (provided by M. Yamamoto, University of Tokyo) into *ura4*⁺ by transformation with the PCR-synthesized *ura4*⁺ fragment, as described previously.¹² Then, KAY587 was created by introducing *int6*Δ by transformation with the PCR-synthesized *int6*Δ:*kanMX* fragment, as described previously.²³

Table 3. Strains used in this study

Strains	Genotype (reference if constructed previously)
<i>SP223 derivatives</i>	
WY764	<i>h⁻ ade6-M216 leu1-32::leu1⁺ ura4-D18Δura4⁺</i> ¹⁰
KAY252	<i>h⁻ ade6-M216 leu1-32::leu1⁺ ura4-D18Δura4⁺ int6Δ::kanMX¹²</i>
KAY406	<i>h⁻ ade6-M216 leu1-32::leu1⁺ (pJK148) ura4-D18 gcn2Δ::ura4⁺</i> ¹²
<i>JY878 derivatives</i>	
KAY456	<i>h⁹⁰ ade6-M216 leu1-32::leu1⁺ (pJK148) ura4-D18::ura4⁺</i> ¹²
KAY508	<i>h⁹⁰ ade6-M216 leu1-32::leu1⁺ (pJK148) ura4-D18::ura4⁺ int6ΔkanMX¹²</i>
<i>JY879 derivatives</i>	
KAY586	<i>h⁹⁰ ade6-M210 leu1-32 ura4-D18 ura4⁺</i>
KAY587	<i>h⁹⁰ ade6-M210 leu1-32 ura4-D18 ura4⁺ int6ΔkanMX</i>
<i>PR109 derivatives</i>	
KAY641	<i>h⁻ leu1-32::leu1⁺ (pJK148) ura4-D18::ura4⁺</i> ¹²
KAY647	<i>h⁻ leu1-32::leu1⁺ (pJK148) ura4-D18::ura4⁺ int6ΔkanMX¹²</i>
KAY640	<i>h⁻ leu1-32::leu1⁺ (pJK148) ura4-D18 sty1Δ::ura4⁺</i> ¹²
KAY649	<i>h⁻ leu1-32::leu1⁺ (pJK148) ura4-D18 eif3hΔ::ura4⁺</i>
KAY793	<i>h⁻ leu1-32 ura4-D18 sty1-His₆HA::ura4⁺ wis1-MycΔura4⁺ p(leu1⁺)</i>
KAY794	<i>h⁻ leu1-32 ura4-D18 sty1-His₆HA::ura4⁺ mcs4Δura4⁺ p(leu1⁺)</i>
<i>Miscellaneous</i>	
JP3	<i>h⁻⁵²</i>
JP260	<i>h⁺ wis1Δ kanMX⁵²</i>
JP436	<i>h⁺ ade6-M210 ura4-D18 sui2-S51A::ura4⁺</i> ³³
KAY852	<i>h⁹⁰ ade6-M210 leu1-32 ura4-D18 his7-366 wis4::ura4⁺ p(leu1⁺) p(his7⁺)</i>

Reference is indicated if the genotype had been constructed previously.

Yeast media

We used the complex-rich YES medium and the defined EMM throughout our study.⁶⁰ To study histidine starvation by the addition of 3AT, we omitted histidine in the media and used minimal EMM or complete EMM supplemented with amino acids and other nutrients but lacking histidine (EMM-C-His), as described previously.¹² To study the effect of NAC (O1049; Fisher Chemical), we used minimal EMM supplemented with adenine (EMM + Ade) or EMM dropout with complete amino acids and other supplements, as described previously.¹² We determined that NAC was effective when its concentration was four to five times higher than that of 3AT in the EMM + Ade medium. Thus, 40 mM NAC was supplemented with the EMM + Ade medium containing 10 mM 3AT. Likewise, 120 mM NAC was supplemented with the EMM + Ade medium containing 30 mM 3AT. To add these NAC concentrations to the EMM, we prepared a stock solution of NAC in EMM to a final concentration of

500 mM, which was then neutralized to pH 5.6 by KOH and filter sterilized.

Yeast growth and viability assays

Yeast cells were grown at a permissive temperature of 30 °C throughout the study. To determine the titer of yeast for both drug sensitivity assay and viability assay, we spotted 5 μ l of 0.15 A_{600} units of culture, or 10-fold and 100-fold dilutions of this culture preparation, onto the agar plates and incubated the plates at 30 °C. For 3AT sensitivity assays, spotted cultures were incubated in a medium containing the indicated concentrations of 3AT, NAC, and histidine. For the viability assays following 3AT-induced histidine starvation, fresh overnight cultures of yeast were inoculated into ~3 ml of liquid EMM + Ade medium with the indicated concentrations of NAC, histidine, and 3AT. The cultures were initiated at an A_{600} of ~0.3 with constant agitation at 30 °C, and aliquots were periodically removed to measure the absorbance at 600 nm, which was subsequently plotted against growth time. Additionally, serially diluted cultures were spotted onto the YES agar plates, incubated at 30 °C for 2 days, and photographed. Colonies formed on each spot were counted to determine viability, as presented by CFU/ A_{600} . If two or more serially diluted spots contained well-dispersed colonies, the CFU/ A_{600} values obtained from each spot were averaged to determine the viability for that condition. Three independent viability assays were performed.

For viability assays with H₂O₂, cells were grown to an A_{600} of 0.5, and then H₂O₂ was added at different final concentrations. After treatment for 4 h, the culture was withdrawn, diluted, and spotted onto YES plates, and the plates were incubated for 2 days.

Biochemical and molecular biology methods

Standard biochemical, genetic, and molecular biology techniques were used throughout the study. Northern and Western blot assays were performed as described previously,¹² using ³²P probes generated by PCR with the pairs of primers listed in Table 4 and affinity-purified anti-Atf1 antibodies,¹⁵ respectively. The total protein synthesis rate was measured by [³⁵S]methionine incorporation, also as described previously.¹⁵ Statistical analyses used *t* test.

To perform an analysis of nucleosome structures, we partially digested crude chromatin fractions from 3AT-treated cells with 0 U/ml, 20 U/ml, or 30 U/ml MNase, and we purified the DNA for complete HpaII digestion and gel electrophoresis.³⁵ The position of MNase cleavage was determined by Southern blot hybridization on the cleavage products using [³²P]DNA probe specific for a part of the *cta3⁺* coding region. Primers used to amplify the labeled probe are listed in Table 4. To confirm Atf1 binding to the *cta3⁺* CRE, we performed chromatin immunoprecipitation using a strain encoding Atf1-HA and anti-HA antibodies, essentially as described previously.¹⁴ Briefly, the area of *cta3* CRE bound to Atf1-HA was immunoprecipitated with anti-HA antibodies and detected by quantitative real-time PCR with the primers listed in Table 4.

Table 4. List of oligodeoxyribonucleotides used in this study

Name	Nucleotide sequences (5'–3')	Gene
Primers designed to create and confirm the strains deleted for <i>eif3h</i> ⁺		
1	eIF3h-FW TAGAAAAGGTTTAAATAAACTGGTAGG CTCCTCTATTCTATAACTTGTAATCGCC GACAGCCATGGCTTTAAAAAGTTGCCG GATCCCCGGGTTAATTA	<i>eif3h</i>
2	eIF3h-RV TTAAGTAGATCCTTTTATTTTAAATGCTAC GAGGTATAACTAGTGAGAGTGAAGAAGA ATGCTCCATTTTTTATAAACAAGAATTC GAGCTCGTTTAAAC	<i>eif3h</i>
3	eIF3h-up GAGCTTAAGGCCGAGAAAAC	<i>eif3h</i>
4	eIF3h-down TATGCTGTATCAAGAAAACC	<i>eif3h</i>
5	ura4-midF GTGTGTACTTTGAAAGTCTAGCTTTA	<i>ura4</i>
6	ura4-midR CCTGTATAATACCCTCGCC	<i>ura4</i>
Primers designed by Lyne <i>et al.</i> in their microarray studies ⁶¹		
7	2-A11_C418.01c_his4_F TAGAGAACTCCTTTGGCGGA	<i>his4</i>
8	2-A11_C418.01c_his4_R CAACTTCGACAGCAGGATGA	<i>his4</i>
9	20-G9_arg3_F TCTCCAGGCGTTAGCAGATT	<i>arg3</i>
10	20-G9_arg3_R TGCATGAATTTGCAGCTAGG	<i>arg3</i>
11	2-E7_C1105.02c_lys4_F CAACCGTGTGGTATTGCTG	<i>lys4</i>
12	2-E7_C1105.02c_lys4_R GCGACAAGGTTTTCAAGCTC	<i>lys4</i>
13	53-F9_atf1 mts1 sss1 gad7_F ACCCTACTGGAGCTGGATT	<i>atf1</i>
14	53-F9_atf1 mts1 sss1 gad7_R TACCTGTAACAGCTTGGGGG	<i>atf1</i>
15	27-H10_pcr1 mts2_F CGTCTCTAAATTTGCCAGA	<i>pcr1</i>
16	27-H10_pcr1 mts2_R GGTGTTGATTGGAGGGAGA	<i>pcr1</i>
17	33-G9_gpd1_F GGTGTAGTTGGCTCCGGTAA	<i>gpd1</i>
18	33-G9_gpd1_R TCTCACAGAATTGCTCACGG	<i>gpd1</i>
19	12-F1_cta1_F TCGTGATCCCCGCTAAATC	<i>cta1</i>
20	12-F1_cta1_R AAGGTAAGCGTCCAACCCT	<i>cta1</i>
Primers designed by Hirota <i>et al.</i> (see Fig. 7c)		
21	cta3 ORF-5' CGAACATTGGCTTCTCC	<i>cta3</i>
22	cta3 ORF-3' GGTGCGTAACAAATTC	<i>cta3</i>
23	cta3 CRE-5' TAACAACACTCCGCCATTCG	<i>cta3</i>
24	cta3 CRE-3' TGACTCCGACATTGATTTCCT	<i>cta3</i>

Microarray analysis

Microarray data generated previously¹² were reanalyzed in GeneSpring (Agilent Technologies, Palo Alto, CA). The significance of overlap between different gene lists was calculated in GeneSpring using standard Fisher's exact test, and *p* values were adjusted with Bonferroni multiple testing correction.

Acknowledgements

We thank E. Boye, C. Hoffman, J. Millar, J. Petersen, K. Shiozaki, Y. Watanabe, and M. Yamamoto for the timely gift of materials; K. Hall, Y. Ikeda, and R. Welti for sharing their results before publication; and H. Kurata and H. Masai for a stimulating discussion. This work was supported by pilot grant P20 RR016475 from the Kansas IDeA Network of Biomedical Research Excellence, National Institutes of Health Center for Research Resources; an innovative award from the Kansas State University Terry Johnson Cancer Center; National Institutes of Health grant GM67481 (to K.A.); and National Institutes of Health grant GM49164 (to R.C.W.).

Supplementary Data

Supplementary data associated with this article can be found, in the online version, at [doi:10.1016/j.jmb.2010.09.016](https://doi.org/10.1016/j.jmb.2010.09.016)

References

- Dever, T. E., Dar, A. C. & Sicheri, F. (2007). The eIF2 α kinase. In *Translational Control in Biology and Medicine* (Mathews, M. B., Sonenberg, N. & Hershey, J. W. B., eds), pp. 319–344, Cold Spring Harbor Laboratory Press, Cold Spring Harbor, NY.
- Schneider, R. J. & Sonenberg, N. (2007). Translational control in cancer development and progression. In *Translational Control in Biology and Medicine* (Mathews, M. B., Sonenberg, N. & Hershey, J. W. B., eds), pp. 401–431, Cold Spring Harbor Laboratory Press, Cold Spring Harbor, NY.
- Martindale, J. L. & Holbrook, N. J. (2003). Cellular response to oxidative stress: signaling for suicide and survival. *J. Cell. Physiol.* **192**, 1–15.
- Bi, M., Naczki, C., Koritzinsky, M., Fels, D., Blais, J., Hu, N. *et al.* (2005). ER stress-regulated translation increases tolerance to extreme hypoxia and promotes tumor growth. *EMBO J.* **24**, 3470–3481.
- Liu, L., Wise, D. R., Diehl, J. A. & Simon, M. C. (2008). Hypoxic reactive oxygen species regulate the

- integrated stress response and cell survival. *J. Biol. Chem.* **283**, 31153–31162.
6. Harding, H. P., Zhang, Y., Zeng, H., Novoa, I., Lu, P. D., Calton, M. *et al.* (2003). An integrated stress response regulates amino acid metabolism and resistance to oxidative stress. *Mol. Cell*, **11**, 619–633.
 7. Ye, J. & Koumenis, C. (2009). ATF4, an ER stress and hypoxia-inducible transcription factor and its potential role in hypoxia tolerance and tumorigenesis. *Curr. Mol. Med.* **9**, 411–416.
 8. Blais, J. D., Addison, C. L., Edge, R., Falls, T., Zhao, H., Wary, K. *et al.* (2006). PERK-dependent translational regulation promotes tumor cell adaptation and angiogenesis in response to hypoxic stress. *Mol. Cell. Biol.* **26**, 9519–9532.
 9. Zhan, K., Vattem, K. M., Bauer, B. N., Dever, T. E., Chen, J. J. & Wek, R. C. (2002). Phosphorylation of eukaryotic initiation factor 2 by heme-regulated inhibitor kinase-related protein kinases in *Schizosaccharomyces pombe* is important for resistance to environmental stress. *Mol. Cell. Biol.* **22**, 7134–7146.
 10. Zhan, K., Narasimhan, J. & Wek, R. C. (2004). Differential activation of eIF2 kinases in response to cellular stresses in *Schizosaccharomyces pombe*. *Genetics*, **168**, 1867–1875.
 11. Natarajan, K., Meyer, M. R., Jackson, B. M., Slade, D., Roberts, C., Hinnebusch, A. G. & Marton, M. J. (2001). Transcriptional profiling shows that Gcn4p is a master regulator of gene expression during amino acid starvation in yeast. *Mol. Cell. Biol.* **21**, 4347–4368.
 12. Udagawa, T., Nemoto, N., Wilkinson, C., Narashimhan, J., Watt, S., Jiang, L. *et al.* (2008). Int6/eIF3e promotes general translation and Atf1 abundance to modulate Sty1 MAP kinase-dependent stress response in fission yeast. *J. Biol. Chem.* **283**, 22063–22075.
 13. Ikner, A. & Shiozaki, K. (2005). Yeast signaling pathways in the oxidative stress response. *Mutat. Res.* **569**, 13–27.
 14. Reiter, W., Watt, S., Dawson, K., Lawrence, C. L., Bähler, J., Jones, N. & Wilkinson, C. R. M. (2008). Fission yeast MAP kinase Sty1 is recruited to stress-induced genes. *J. Biol. Chem.* **283**, 9945–9956.
 15. Lawrence, C. L., Maekawa, H., Worthington, J. L., Reiter, W., Wilkinson, C. R. M. & Jones, N. (2007). Regulation of *Schizosaccharomyces pombe* Atf1 protein levels by Sty1-mediated phosphorylation and heterodimerization with Pcr1. *J. Biol. Chem.* **282**, 5160–5170.
 16. Chen, D., Toone, W. M., Mata, J., Lyne, R., Burns, G., Kivinen, K. *et al.* (2003). Global transcriptional response of fission yeast to environmental stress. *Mol. Biol. Cell*, **14**, 214–229.
 17. Marchetti, A., Buttitta, F., Miyazaki, S., Gallahan, D., Smith, G. H. & Callahan, R. (1995). *Int-6*, a highly conserved, widely expressed gene, is mutated by mouse mammary tumor virus in mammary preneoplasia. *J. Virol.* **69**, 1932–1938.
 18. Asano, K., Merrick, W. C. & Hershey, J. W. B. (1997). The translation initiation factor eIF3-p48 subunit is encoded by *int-6*, a site of frequent integration by the mouse mammary tumor virus genome. *J. Biol. Chem.* **272**, 23477–23480.
 19. Hinnebusch, A. G., Dever, T. E. & Asano, K. (2007). Mechanism of translation initiation in the yeast *Saccharomyces cerevisiae*. In *Translational Control in Biology and Medicine* (Mathews, M. B., Sonenberg, N. & Hershey, J. W. B., eds), pp. 225–268, Cold Spring Harbor Laboratory Press, Cold Spring Harbor, NY.
 20. Rasmussen, S. B., Kordon, E., Callahan, R. & Smith, G. H. (2001). Evidence for the transforming activity of a truncated Int6 gene, *in vitro*. *Oncogene*, **20**, 5291–5301.
 21. Mayeur, G. L. & Hershey, J. W. B. (2002). Malignant transformation by the eukaryotic translation initiation factor 3 subunit p48 (eIF3e). *FEBS Lett.* **514**, 49–64.
 22. Mack, D. L., Boulanger, C. A., Callahan, R. & Smith, G. H. (2007). Expression of truncated Int6/eIF3e in mammary alveolar epithelium leads to persistent hyperplasia and tumorigenesis. *Breast Cancer Res.* **9**, R42.
 23. Akiyoshi, Y., Clayton, J., Phan, L., Yamamoto, M., Hinnebusch, A. G., Watanabe, Y. & Asano, K. (2001). Fission yeast homolog of murine Int-6 protein, encoded by mouse mammary tumor virus integration site, is associated with the conserved core subunits of eukaryotic translation initiation factor 3. *J. Biol. Chem.* **276**, 10056–10062.
 24. Zhou, C., Arslan, F., Wee, S., Krishnan, S., Ivanov, A. R., Oliva, A. *et al.* (2005). PCI proteins eIF3e and eIF3m define distinct translation initiation factor 3 complexes. *BMC Biol.* **3**, 14.
 25. Sha, Z., Brill, L. M., Cabrera, R., Kleefeld, O., Scheliga, J. S., Glickman, M. H. *et al.* (2009). The eIF3 interactome reveals the translatome, a supercomplex linking protein synthesis and degradation machineries. *Mol. Cell*, **36**, 142–152.
 26. LeFebvre, A. K., Korneeva, N. L., Trutschl, M., Cvek, U., Duzan, R. D., Bradley, C. A. *et al.* (2006). Translation initiation factor eIF4G-1 binds to eIF3 through the eIF3e subunit. *J. Biol. Chem.* **281**, 22917–22932.
 27. Masutani, M., Sonenberg, N., Yokoyama, S. & Imataka, H. (2007). Reconstitution reveals the functional core of mammalian eIF3. *EMBO J.* **26**, 3373–3383.
 28. Ueda, M., Kinoshita, H., Yoshida, T., Kamasawa, N., Osumi, M. & Tanaka, A. (2003). Effect of catalase-specific inhibitor 3-amino-1,2,4-triazole on yeast peroxisomal catalase *in vivo*. *FEMS Microbiol. Lett.* **219**, 93–98.
 29. Kanoh, J., Watanabe, Y., Ohsugi, M., Iino, Y. & Yamamoto, M. (1996). *Schizosaccharomyces pombe gad7⁺* encodes a phosphoprotein with a bZIP domain, which is required for proper G1 arrest and gene expression under nitrogen starvation. *Genes Cells*, **1**, 391–408.
 30. Sansó, M., Gogol, M., Ayté, J., Seidel, C. & Hidalgo, E. (2008). Transcription factors Pcr1 and Atf1 have distinct roles in stress- and Sty1-dependent gene regulation. *Eukaryotic Cell*, **7**, 826–835.
 31. Ohmiya, R., Yamada, H., Nakashima, K., Aiba, H. & Mizuno, T. (1995). Osmoregulation of fission yeast: cloning of two distinct genes encoding glycerol-3-phosphate dehydrogenase, one of which is responsible for osmotolerance for growth. *Mol. Microbiol.* **18**, 963–973.
 32. Morigasaki, S., Shimada, K., Ikner, A., Yanagida, M. & Shiozaki, K. (2008). Glycolytic enzyme GAPDH promotes peroxide stress signaling through multistep

- phosphorelay to a MAPK cascade. *Mol. Cell*, **30**, 108–113.
33. Tvegård, T., Soltani, H., Skjølberg, H. C., Krohn, M., Nilssen, E. A., Kearsley, S. E. *et al.* (2007). A novel checkpoint mechanism regulating the G1/S transition. *Genes Dev.* **21**, 649–654.
 34. Shiozaki, K. & Russell, P. (1995). Cell-cycle control linked to extracellular environment by MAP kinase pathway in fission yeast. *Nature*, **378**, 739–743.
 35. Hirota, K., Hasemi, T., Yamada, T., Mizuno, K. I., Hoffman, C. S., Shibata, T. & Ohta, K. (2004). Fission yeast global repressors regulate the specificity of chromatin alteration in response to distinct environmental stresses. *Nucleic Acids Res.* **32**, 855–862.
 36. Chung, W. H., Kim, K. D. & Roe, J. H. (2005). Localization and function of three monothiol glutaredoxins in *Schizosaccharomyces pombe*. *Biochem. Biophys. Res. Commun.* **330**, 604–610.
 37. Deshpande, G. P., Hayles, J., Hoe, K. L., Kim, D. U., Park, H. O. & Hartsuiker, E. (2009). Screening a genome wide *S. pombe* deletion library identifies novel genes and pathways involved in the DNA damage response. *DNA Repair*, **8**, 672–679.
 38. Kaur, J. & Bachhawat, A. K. (2007). Ycy1p, a novel, high-affinity, cysteine-specific transporter from the yeast *Saccharomyces cerevisiae*. *Genetics*, **176**, 877–890.
 39. Oxelmark, E., Marchini, A., Malanchi, I., Magherini, F., Jaquet, L., Hajibagheri, M. A. *et al.* (2000). Mmf1p, a novel yeast mitochondrial protein conserved throughout evolution and involved in maintenance of the mitochondrial genome. *Mol. Cell. Biol.* **20**, 7784–7797.
 40. Kispal, G., Csere, P., Prohl, C. & Lill, R. (1999). The mitochondrial proteins Atm1p and Nfs1p are essential for biogenesis of cytosolic Fe/S proteins. *EMBO J.* **14**, 3981–3989.
 41. Chen, D., Wilkinson, C. R. M., Watt, S., Penkett, C. J., Toone, W. M., Jones, N. & Bähler, J. (2008). Multiple pathways differentially regulate global oxidative stress responses in fission yeast. *Mol. Biol. Cell*, **19**, 308–317.
 42. Dunand-Sauthier, I., Walker, C. A., Narashimhan, J., Pearce, A. K., Wek, R. C. & Humphrey, T. C. (2005). Stress-activated protein kinase pathway functions to support protein synthesis and translational adaptation in response to environmental stress in fission yeast. *Eukaryotic Cell*, **4**, 1785–1793.
 43. Fukuzawa, K., Fujisaki, A., Akai, K., Tokumura, A., Terao, J. & Gebicki, J. M. (2006). Measurement of phosphatidylcholine hydroperoxides in solution and in intact membranes by the ferric-xylene orange assay. *Anal. Biochem.* **359**, 18–25.
 44. Mitchell, A., Romano, G. H., Groisman, B., Yona, A., Dekel, E., Kupiec, M. *et al.* (2009). Adaptive prediction of environmental changes by microorganisms. *Nature*, **460**, 220–224.
 45. Shiozaki, K., Shiozaki, M. & Russell, P. (1997). Mcs4 mitotic catastrophe suppressor regulates the fission yeast cell cycle through the Wik1-Wis1-spc1 kinase cascade. *Mol. Biol. Cell*, **8**, 409–419.
 46. Wilhelm, B., Marguerat, S., Watt, S., Schubert, F., Wood, V., Goodhead, I. *et al.* (2008). Dynamic repertoire of a eukaryotic transcriptome surveyed at single-nucleotide resolution. *Nature*, **453**, 1239–1243.
 47. Asano, K., Vornlocher, H. P., Richter-Cook, N. J., Merrick, W. C., Hinnebusch, A. G. & Hershey, J. W. B. (1997). Structure of cDNAs encoding human eukaryotic initiation factor 3 subunits: possible roles in RNA binding and macromolecular assembly. *J. Biol. Chem.* **272**, 27042–27052.
 48. Zhou, M., Sandercock, A. M., Fraser, C. S., Ridlova, G., Stephens, E., Schenauer, M. R. *et al.* (2008). Mass spectrometry reveals modularity and a complete subunit interaction map of the eukaryotic translation factor eIF3. *Proc. Natl Acad. Sci. USA*, **105**, 18139–18144.
 49. Takemaru, K., Harashima, S., Ueda, H. & Hirose, S. (1998). Yeast coactivator MBF1 mediates GCN4-dependent transcriptional activation. *Mol. Cell. Biol.* **18**, 4971–4976.
 50. Cherkasova, V. A. & Hinnebusch, A. G. (2003). Translational control by TOR and TAP42 through dephosphorylation of eIF2 kinase GCN2. *Genes Dev.* **17**, 859–872.
 51. Staschke, K. A., Dey, S., Zaborske, J. M., Palam, L. R., McClintick, N. J., Pan, T. *et al.* (2010). Integration of general amino acid control and TOR regulatory pathways in nitrogen assimilation in yeast. *J. Biol. Chem.* **285**, 16893–16911.
 52. Petersen, J. & Nurse, P. (2007). TOR signalling regulates mitotic commitment through the stress MAP kinase pathway and the Polo and Cdc2 kinases. *Nat. Cell Biol.* **9**, 1–10.
 53. Thiaville, M. M., Pan, Y. X., Gjymishka, A., Zhong, C., Kaufman, R. J. & Kilberg, M. S. (2008). MEK signaling is required for phosphorylation of eIF2 α following amino acid limitation of HepG2 human hepatoma cells. *J. Biol. Chem.* **283**, 10848–10857.
 54. Kennedy, N. J., Cellurale, C. & Davis, R. J. (2007). A radical role for p38 MAPK in tumor initiation. *Cancer Cell*, **11**, 101–103.
 55. Dolado, I., Swat, A., Ajenjo, N., De Vita, G., Cuadrado, A. & Nebreda, A. R. (2007). p38 α MAP kinase as a sensor of reactive oxygen species in tumorigenesis. *Cancer Cell*, **11**, 191–205.
 56. Shiozaki, K., Shiozaki, M. & Russell, P. (1998). Heat stress activates fission yeast Spc1/Sty1 MAPK by a MEKK-independent mechanism. *Mol. Biol. Cell*, **9**, 1339–1349.
 57. Nguyen, A. N., Lee, A., Place, W. & Shiozaki, K. (2000). Multistep phosphorelay proteins transmit oxidative stress signals to the fission yeast stress-activated protein kinase. *Mol. Biol. Cell*, **11**, 1169–1181.
 58. Shieh, J. C., Wilkinson, M. G. & Millar, J. B. A. (1998). The Win1 mitotic regulator is a component of the fission yeast stress-activated Sty1 MAPK pathway. *Mol. Biol. Cell*, **9**, 311–322.
 59. Bähler, J., Wu, J. Q., Longtine, M. S., Shah, N. G., McKenzie, A., III, Steever, A. B. *et al.* (1998). Heterologous modules for efficient and versatile PCR-based gene targeting in *Schizosaccharomyces pombe*. *Yeast*, **14**, 943–951.
 60. Moreno, S., Klar, A. & Nurse, P. (1991). Molecular genetic analysis of the fission yeast *Schizosaccharomyces pombe*. *Methods Enzymol.* **194**, 795–823.
 61. Lyne, R., Burns, G., Mata, J., Penkett, C. J., Rustici, G., Chen, D. *et al.* (2003). Whole-genome microarrays of fission yeast: characteristics, accuracy, reproducibility, and processing of array data. *BMC Genomics*, **4**, 27.